Surface-enhanced second-harmonic generation of optical beams from a metal surface

Guifang Li and S. R. Seshadri
Department of Electrical and Computer Engineering, University of Wisconsin–Madison, Madison, Wisconsin 53706-1691
(Received 4 February 1991)

The spatiotemporal behavior of the surface-enhanced second-harmonic generation at a metal-vacuum interface with a sinusoidal grating is investigated. Using a singular-perturbation approach, the effects of self-phase modulation and the nonlinear excitation of the surface polariton on the enhanced second-harmonic generation are taken into account. The intensity dependence of the enhancement factor is presented. Lateral shift and beam-profile modification are predicted in the second-harmonic radiation.

I. INTRODUCTION

Surface-enhanced optical effects mediated by surface polaritons such as second-harmonic generation,[1–4] hot-electron generation,[5] Brillouin scattering,[6] Raman scattering,[7] photoconductivity in metal-oxide-metal tunnel junction,[8] and optical bistability[9] have attracted considerable attention in recent years. Since the observation of the surface-enhanced second-harmonic generation at a rough silver-air interface,[1] theoretical effort has been devoted to the quantitative analysis of this phenomenon.[2–4] In these treatments, the exact model of the rough metal-air interface was not used because of the difficulties caused by the nonlinearities in the metal. The deterministic model of the sinusoidal surface profile[10] was adopted instead. The limitation of these previous investigations include the plane-wave assumption of the incident wave. Furthermore, the effect of spatiotemporal evolution[11] and the nonlinear effects in the excitation[12] of the surface polariton, the agent responsible for the surface-enhanced second-harmonic generation, have not been taken into account. These effects are important in this study for the following reasons. Due to the nonlinearities in the metal, the amplitude of the surface polariton undergoes self-phase modulation directly resulting in the spatiotemporal variation of the strength of the second-harmonic radiation in vacuum. Also, we have previously found that the efficiency of the excitation of the nonlinear surface polariton is a function of the width and the intensity of the incident beam. Therefore, it is expected that the efficiency of the surface-enhanced second-harmonic generation is also a function of the width and the intensity of the incident beam.

In this paper we improve the previous analyses of the surface-enhanced second-harmonic generation at a sinusoidal metal-air interface by including the effects of the finite width of the incident beam and the self-phase modulation and nonlinear excitation of the surface polariton. The nonlinearities in the metal are included systematically using the hydrodynamic model, then treated perturbatively. The amplitude of the sinusoidal surface corrugation is also considered as a small parameter. The method of reduced Rayleigh equations was employed previously[4] so that it is not necessary to treat the amplitude of the grating as a small perturbation. However, it is generally adequate to assume that the amplitude of the grating is small because it is used to model the rough surface and because only small-amplitude grating can ensure the efficient excitation of the surface polariton in the experiments.[13]

The paper is organized as follows. The formulation of the problem is given in Sec. II. In Sec. III the perturbation expansions of the governing equations and the boundary conditions are discussed. The self-phase modulation and the excitation of the nonlinear surface polariton are summarized in Sec. IV. The strength of the surface-enhanced second-harmonic generation in various directions is determined in Sec. V. Section VI presents some illustrative numerical results on the enhancement factor and beam properties of the surface-enhanced second-harmonic generation by the sinusoidal surface. Some concluding remarks are given in Sec. VII.

II. FORMULATION OF THE PROBLEM

A. Geometry

We consider second-harmonic generation from an interface $x=f(z)$ separating the half-space $x>f(z)$ of vacuum from the half-space $x<f(z)$ of free-electron metal. For a planar interface $f(z)$ is a constant $[x=f(z)=0$, without loss of generality]; the incident quasi-plane-wave of fundamental frequency ω upon reflection generates an evanescent wave into the metal which decays away from the interface. The nonlinearities in the free-electron metal produce collective electron motion at the second-harmonic frequency, which in turn excites second-harmonic electromagnetic fields in the metal and vacuum. When the interface is sinusoidally and weakly corrugated (see Fig. 1), the profile of the surface is given by $x=f(z)=\delta\eta\cos Kz$, where δ is used to indicate the smallness of the amplitude η of the corrugation, and K is the wave number of the corrugation. The incident fundamental quasi-plane-wave then not only generates an evanescent wave into the metal but also excites an electromagnetic surface wave called the surface polariton for a suitable value of K. The surface polariton transports energy along the interface with its fields also concentrat-

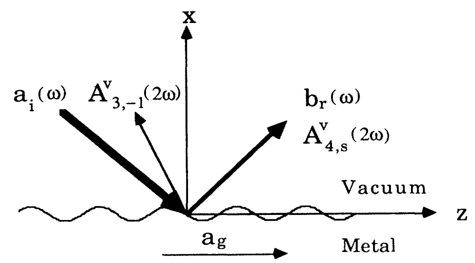

FIG. 1. Geometry for the surface-enhanced second-harmonic generation. a_i, the normalized amplitude of the incident wave; b_r, the normalized amplitude of the reflected wave at the fundamental frequency; a_g, the amplitude of the surface polariton; $A^v_{3,-1}$, normalized amplitude of the second-harmonic radiation in the -1 diffraction order; $A^v_{4,s}$, the normalized amplitude of the second-harmonic radiation in the specular direction.

ed near the interface. However, in the metal region, the energy transported in the surface polariton is orders of magnitude larger than that transported in the evanescent wave transmitted through the planar interface. The intense surface-polariton fields produce a strong collective electron motion at the second-harmonic frequency giving rise to the surface-polariton-mediated second-harmonic generation. This second-harmonic generation is known as the surface-enhanced second-harmonic generation since it is relatively more intense than that obtained directly without the intermediary of the surface polariton. We calculate the efficiencies of the second-harmonic generation at the planar interface and the sinusoidally corrugated interface and subsequently determine the enhancement factor by the corrugated interface. When the incident waves are nearly plane waves of finite extent, some interesting beam properties are also present.

B. Governing equations

Electromagnetic wave phenomena are governed by Maxwell's equations and the material equations of the supporting media. The nonlinear properties of the free-electron metal have been previously accounted for by the introduction of the nonlinear polarization.[14] This approach, however, cannot be used to correctly quantify the efficiency of the second-harmonic generation of nonplanar incident waves and the effects of the nonlinear evolution of the surface polariton on the efficiency of the surface-enhanced second-harmonic generation. Hence, we include systematically the nonlinearities of the free-electron metal in a general manner through the relativistically correct hydrodynamic equations.[11,12]

The equilibrium electron density is denoted by N_0. We introduce a standard electric field $E_0 = m_e c \omega_p / e$, where m_e is the effective rest mass of an electron, $-e$ is the electronic charge, c is the velocity of electromagnetic wave in free space, and ω_p is the proper plasma angular frequency of the conduction electrons. We normalize the electron number density by N_0, the electric field by E_0, the magnetic flux density by E_0/c, the time by $1/\omega_p$, the distance by c/ω_p, and the velocity by c. Let $\mathbf{E}^v$ and $\mathbf{B}^v$ be the normalized electric field and magnetic flux density, respectively, in vacuum, and let N, $\mathbf{V}$, $\mathbf{E}^m$, and $\mathbf{B}^m$ be the normalized number density and velocity of electrons, the electric field, and the magnetic flux density, respectively, in the metal. The electromagnetic wave motions are governed by the following equations:

$$\nabla \times \mathbf{E}^v = -\frac{\partial}{\partial t}\mathbf{B}^v , \tag{1}$$

$$\nabla \times \mathbf{B}^v = \frac{\partial}{\partial t}\mathbf{E}^v , \tag{2}$$

for the vacuum,

$$\nabla \times \mathbf{E}^m = -\frac{\partial}{\partial t}\mathbf{B}^m , \tag{3}$$

$$\nabla \times \mathbf{B}^m = \frac{\partial}{\partial t}\mathbf{E}^m - N\mathbf{V} , \tag{4}$$

$$\frac{\partial N}{\partial t} + \nabla \cdot (N\mathbf{V}) = 0 , \tag{5}$$

$$\left[\frac{\partial}{\partial t} + \mathbf{V}\cdot\nabla\right][(1-V^2)^{1/2}\mathbf{V}] = -(\mathbf{E}^m + \mathbf{V}\times\mathbf{B}^m) , \tag{6}$$

for the metal. Equations (4)–(6) are nonlinear. Equations (5) and (6) are, respectively, the nonlinear equations of continuity and motion. The electromagnetic wave motions also have to satisfy the boundary conditions that the tangential components of the electric and magnetic fields be continuous at the interface.

III. PERTURBATION EXPANSIONS

Small parameters occur naturally in the problem under consideration. The electromagnetic wave introduces a small (compared to N_0) space-time variation of the electron number density which is otherwise uniform. The nonlinear responses (high harmonics) in the variation are small compared to the variation of the electron number density at the fundamental frequency. Hence, the high-harmonic electromagnetic waves are also significantly weaker than the incident wave at the fundamental frequency. The nonlinear wave phenomena such as the self-phase modulation of the nonlinear surface polariton take place at longer space and time scale than the wavelength and the period of the fundamental electromagnetic wave. Finally, the amplitude η of the surface corrugation is also a small parameter as compared to the wavelength. The physical occurrence of these small parameters suggests the application of the multiple-scale singular perturbation technique.

To this end, we introduce multiple time scales t_n and multiple space scales x_n and z_n, where $t_n = \delta^n t$, $x_n = \delta^n x$, and $z_n = \delta^n z$. The geometry is invariant with respect to the y direction. We therefore assume that the problem is invariant in y. The various field quantities are also expanded as power series in δ: $\mathbf{E}^i = \sum \delta^s \mathbf{E}^i_s$, $\mathbf{B}^i = \sum \delta^s \mathbf{B}^i_s$, for $i = v, m$, $N = 1 + \sum \delta^s N_s$, $\mathbf{V} = \sum \delta^s \mathbf{V}_s$. Also, according to the chain rule of differentiation, $\partial/\partial t = \sum \delta^{(s-1)} \partial/\partial t_{(s-1)}$, $\partial/\partial x = \sum \delta^{(s-1)} \partial/\partial x_{(s-1)}$, and $\partial/\partial z$

$=\sum\delta^{(s-1)}\partial/\partial z_{(s-1)}$, where $\partial/\partial t_s$, $\partial/\partial x_s$, and $\partial/\partial z_s$ are of order of unity. All the summations in the expansions run over positive integers. Substituting these expansions into Eqs. (1)–(6), writing all the terms as power series of δ, and equating separately the coefficients of various powers of δ, we deduce the set of equations of various orders $O(\delta^s)$. In the first order $O(\delta)$, the problem is linear. The fields separate into two groups, namely the transverse magnetic (TM) mode with fields $B^i_{y1}, E^i_{x1}, E^i_{z1}$, for $i=v$, m, V_{x1}, V_{z1}, and N_1; and the transverse electric mode with fields $B^i_{x1}, B^i_{z1}, E^i_{y1}$, for $i=v$, m, and V_{y1}. The surface polariton is associated with the TM mode. Since the excitation of the TM mode is responsible for the enhanced second-harmonic generation mediated by the surface polariton, we assume that the incident quasi-plane-wave contains only the field components associated with the TM mode. The two modes are orthogonal in the first order. An inspection of the geometrical symmetry and the nature of the nonlinearities shows that the two modes remain orthogonal in subsequent orders. If the incident wave contains only the fields of the TM mode, the fields generated by the nonlinearities and the geometrical inhomogeneity still remain in the TM mode. This conclusion is also confirmed by the perturbation expansions of the governing equations. The governing equations for the fields of the TM mode in various orders are as follows:

$$-\frac{\partial}{\partial t_0}B^v_{ys}-\frac{\partial}{\partial z_0}E^v_{xs}+\frac{\partial}{\partial x_0}E^v_{zs}=S_{1s}\ , \tag{7}$$

$$\frac{\partial}{\partial t_0}E^v_{xs}+\frac{\partial}{\partial z_0}B^v_{ys}=S_{2s}\ , \tag{8}$$

$$\frac{\partial}{\partial t_0}E^v_{zs}-\frac{\partial}{\partial x_0}B^v_{ys}=S_{3s}\ , \tag{9}$$

for the vacuum,

$$-\frac{\partial}{\partial t_0}B^m_{ys}-\frac{\partial}{\partial z_0}E^m_{xs}+\frac{\partial}{\partial x_0}E^m_{zs}=S_{4s}\ , \tag{10}$$

$$\frac{\partial}{\partial t_0}E^m_{xs}-V_{xs}+\frac{\partial}{\partial z_0}B^m_{ys}=S_{5s}\ , \tag{11}$$

$$\frac{\partial}{\partial t_0}E^m_{zs}-V_{zs}-\frac{\partial}{\partial x_0}B^m_{ys}=S_{6s}\ , \tag{12}$$

$$\frac{\partial}{\partial t_0}N_s+\frac{\partial}{\partial x_0}V_{xs}+\frac{\partial}{\partial z_0}V_{zs}=S_{7s}\ , \tag{13}$$

$$\frac{\partial}{\partial t_0}V_{xs}+E^m_{xs}=S_{8s}\ , \tag{14}$$

$$\frac{\partial}{\partial t_0}V_{zs}+E^m_{zs}=S_{9s}\ , \tag{15}$$

for the metal. The source terms appearing on the right-hand sides of Eqs. (7)–(15) are equal to zero for $s=1$, and their expressions for $s=2$, 3, and 4 are given in Appendix A.

The governing equations for the magnetic flux density in vacuum and the metal can be derived from Eqs. (7)–(15). In vacuum, substituting E^v_{xs} and E^v_{zs} from Eqs. (8) and (9) into Eq. (7) yields

$$\left[\frac{\partial^2}{\partial x_0^2}+\frac{\partial^2}{\partial z_0^2}-\frac{\partial^2}{\partial t_0^2}\right]B^v_{ys}=\frac{\partial}{\partial t_0}S_{1s}+\frac{\partial}{\partial z_0}S_{2s}-\frac{\partial}{\partial x_0}S_{3s}\ . \tag{16}$$

For the metal region, eliminating V_{xs} from Eq. (11) using Eq. (14) gives E^m_{xs} in terms of B^m_{ys} and the source terms:

$$\left[\frac{\partial^2}{\partial t_0^2}+1\right]E^m_{xs}=-\frac{\partial^2}{\partial z_0\partial t_0}B^m_{ys}+S_{8s}+\frac{\partial}{\partial t_0}S_{5s}\ . \tag{17}$$

A similar manipulation leads to

$$\left[\frac{\partial^2}{\partial t_0^2}+1\right]E^m_{zs}=\frac{\partial^2}{\partial x_0\partial t_0}B^m_{ys}+S_{9s}+\frac{\partial}{\partial t_0}S_{6s}\ . \tag{18}$$

Operating both sides of Eq. (10) by $(\partial^2/\partial t_0^2+1)$ and using Eqs. (17) and (18) lead to

$$\frac{\partial}{\partial t_0}\left[\frac{\partial^2}{\partial x_0^2}+\frac{\partial^2}{\partial z_0^2}-\frac{\partial^2}{\partial t_0^2}-1\right]B^m_{ys}$$
$$=\frac{\partial}{\partial z_0}S_{8s}+\frac{\partial^2}{\partial z_0\partial t_0}S_{5s}-\frac{\partial^2}{\partial x_0^2}S_{9s}-\frac{\partial^2}{\partial x_0\partial t_0}S_{6s}$$
$$+\left[\frac{\partial^2}{\partial t_0^2}+1\right]S_{4s}\ . \tag{19}$$

We now deduce the boundary conditions of various orders. At the interface $x=f(z)$, the tangential components of the magnetic flux density and the electric field B_y and $E_z\cos\theta(z)+E_x\sin\theta(z)$ should be continuous, that is

$$B^v_y=B^m_y\ , \tag{20}$$

$$E^v_z\cos\theta(z)+E^v_x\sin\theta(z)=E^m_z\cos\theta(z)+E^m_x\sin\theta(z)\ , \tag{21}$$

at $x=f(z)$, where

$$\tan\theta(z)=\frac{dx}{dz}=-\delta\eta K\sin Kz\ . \tag{22}$$

In order to exploit fully the smallness of the amplitude of the surface corrugation, we convert the boundary conditions as given by Eqs. (20) and (21) at the actual interface $x=f(z)$ to the equivalent boundary conditions at the average interface $x=0$. The fields in Eqs. (20) and (21) are written as power series in δ, and the fields of each order in δ at the interface $x=f(z)$ are expanded as Taylor series about their values at the average interface $x=0$. When these expressions are substituted into Eqs. (20) and (21), we obtain the equivalent boundary conditions at the average interface $x=0$ as follows:

$$B^v_{y1}=B^m_{y1}\ , \tag{23a}$$

$$E^v_{z1}=E^m_{z1}\ , \tag{23b}$$

for $O(\delta)$,

$$B^{v}_{y2}+\eta\cos Kz_0\frac{\partial}{\partial x_0}B^{v}_{y1}=B^{m}_{y2}+\eta\cos Kz_0\frac{\partial}{\partial x_0}B^{m}_{y1}\ , \tag{24a}$$

$$E^{v}_{z2}+\eta\cos Kz_0\frac{\partial}{\partial x_0}E^{v}_{z1}-\eta K\sin Kz_0(E^{v}_{x1})=E^{m}_{z2}+\eta\cos Kz_0\frac{\partial}{\partial x_0}E^{m}_{z1}-\eta K\sin Kz_0(E^{m}_{x1})\ , \tag{24b}$$

for $O(\delta^2)$,

$$B^{v}_{y3}+\eta\cos Kz_0\left[\frac{\partial}{\partial x_1}B^{v}_{y1}+\frac{\partial}{\partial x_0}B^{v}_{y2}\right]+\tfrac{1}{2}\eta^2\cos^2 Kz_0\left[\frac{\partial^2}{\partial x_0^2}B^{v}_{y1}\right]$$
$$=B^{m}_{y3}+\eta\cos Kz_0\left[\frac{\partial}{\partial x_1}B^{m}_{y1}+\frac{\partial}{\partial x_0}B^{m}_{y2}\right]+\tfrac{1}{2}\eta^2\cos^2 Kz_0\left[\frac{\partial^2}{\partial x_0^2}B^{m}_{y1}\right]\ , \tag{25a}$$

$$E^{v}_{z3}+\eta\cos Kz_0\left[\frac{\partial}{\partial x_1}E^{v}_{z1}+\frac{\partial}{\partial x_0}E^{v}_{z2}\right]+\tfrac{1}{2}\eta^2\cos^2 Kz_0\frac{\partial^2}{\partial x_0^2}E^{v}_{z1}-\eta K\sin Kz_0(E^{v}_{x2})-\eta^2 K\sin Kz_0\cos Kz_0\left[\frac{\partial}{\partial x_0}E^{v}_{x1}\right]$$
$$=E^{m}_{z3}+\eta\cos Kz_0\left[\frac{\partial}{\partial x_1}E^{m}_{z1}+\frac{\partial}{\partial x_0}E^{m}_{z2}\right]+\tfrac{1}{2}\eta^2\cos^2 Kz_0\frac{\partial^2}{\partial x_0^2}E^{m}_{z1}-\eta K\sin Kz_0(E^{m}_{x2})-\eta^2 K\sin Kz_0\cos Kz_0\left[\frac{\partial}{\partial x_0}E^{m}_{x1}\right]\ , \tag{25b}$$

for $O(\delta^3)$,

$$B^{v}_{y4}+\eta\cos Kz_0\left[\frac{\partial}{\partial x_2}B^{v}_{y1}+\frac{\partial}{\partial x_1}B^{v}_{y2}+\frac{\partial}{\partial x_0}B^{v}_{y3}\right]+\tfrac{1}{2}\eta^2\cos^2 Kz_0\left[\frac{\partial^2}{\partial x_0^2}B^{v}_{y2}+2\frac{\partial^2}{\partial x_0\partial x_1}B^{v}_{y1}\right]+\tfrac{1}{6}\eta^3\cos^3 Kz_0\frac{\partial^3}{\partial x_0^3}B^{v}_{y1}$$
$$=B^{m}_{y4}+\eta\cos Kz_0\left[\frac{\partial}{\partial x_2}B^{m}_{y1}+\frac{\partial}{\partial x_1}B^{m}_{y2}+\frac{\partial}{\partial x_0}B^{m}_{y3}\right]$$
$$+\tfrac{1}{2}\eta^2\cos^3 Kz_0\left[\frac{\partial^2}{\partial x_0^2}B^{m}_{y2}+2\frac{\partial^2}{\partial x_0\partial x_1}B^{m}_{y1}\right]+\tfrac{1}{6}\eta^3\cos^2 Kz_0\frac{\partial^3}{\partial x_0^3}B^{m}_{y1}\ , \tag{26a}$$

$$-\eta^2 K\sin Kz_0\cos Kz_0\left[\frac{\partial}{\partial x_0}E^{v}_{x2}+\frac{\partial}{\partial x_1}E^{v}_{x1}\right]-\tfrac{1}{2}\eta^3 K\sin Kz_0\cos^2 Kz_0\frac{\partial^2}{\partial x_0^2}E^{v}_{x1}+\tfrac{1}{2}\eta^2\cos^2 Kz_0\left[\frac{\partial^2}{\partial x_0^2}E^{v}_{z2}+2\frac{\partial^2}{\partial x_0\partial x_1}E^{v}_{z1}\right]$$
$$+\tfrac{1}{6}\eta^3\cos^3 Kz_0\frac{\partial^3}{\partial x_0^3}E^{v}_{z1}+E^{v}_{z4}+\eta\cos Kz_0\left[\frac{\partial}{\partial x_0}E^{v}_{z3}+\frac{\partial}{\partial x_1}E^{v}_{z2}+\frac{\partial}{\partial x_2}E^{v}_{z1}\right]-E^{v}_{x3}\eta K\sin K_{z_0}$$
$$=-\eta^2 K\sin Kz_0\cos Kz_0\left[\frac{\partial}{\partial x_0}E^{m}_{x2}+\frac{\partial}{\partial x_1}E^{m}_{x1}\right]-\tfrac{1}{2}\eta^3 K\sin Kz_0\cos^2 Kz_0\frac{\partial^2}{\partial x_0^2}E^{m}_{x1}+\tfrac{1}{2}\eta^2\cos^2 Kz_0\left[\frac{\partial^2}{\partial x_0^2}E^{m}_{x2}+2\frac{\partial^2}{\partial x_0 x_1}E^{m}_{z1}\right]$$
$$+\tfrac{1}{6}\eta^3\cos^3 Kz_0\frac{\partial^3}{\partial x_0^3}E^{m}_{z1}+E^{m}_{z4}+\eta\cos Kz_0\left[\frac{\partial}{\partial x_0}E^{m}_{z3}+\frac{\partial}{\partial x_1}E^{m}_{z2}+\frac{\partial}{\partial x_2}E^{m}_{z1}\right]-E^{m}_{x3}\eta K\sin Kz_0 \tag{26b}$$

for $O(\delta^4)$. Equations (7)–(15) associated with the equivalent boundary conditions given by Eqs. (23)–(26) are used to investigate the surface-enhanced second-harmonic generation taking into account the self-phase modulation and the nonlinear excitation of the surface polariton. To describe the self-phase modulation and the nonlinear excitation of the surface polariton, it is required to carry out the perturbation procedure up to third order $O(\delta^3)$. The enhanced second-harmonic radiation in the specular direction (see Sec. V) is determined in the fourth order $O(\delta^4)$.

IV. SELF-PHASE MODULATION AND EXCITATION

For the sake of completeness, we briefly summarize the self-phase modulation and the excitation of the nonlinear surface polariton, which are needed in the subsequent evaluation of the enhanced second-harmonic generation. A detailed treatment of these topics is contained in Refs. 11 and 12.

A. Surface polariton

The $O(\delta)$ surface-polariton fields are governed by Eqs. (7)–(15) with $s=1$ for which all the source terms vanish. The $O(\delta)$ magnetic flux densities in vacuum and the metal B^{v}_{y1} and B^{m}_{y1}, are determined from Eqs. (16) and (19) with $s=1$ as

$$B^{v}_{y1}=N_g a_g\exp(-\alpha_v x_0)\exp[i(\beta z_0-\omega t_0)]+\text{c.c.}\ , \tag{27}$$

$$B^{m}_{y1}=N_g a_g\exp(\alpha_m x_0)\exp[i(\beta z_0-\omega t_0)]+\text{c.c.}\ , \tag{28}$$

where the decay coefficients in vacuum and the metal are, respectively,

$$\alpha_v=(\beta^2-\omega^2)^{1/2} , \tag{29a}$$

$$\alpha_m=(\beta^2-\omega^2+1)^{1/2} . \tag{29b}$$

Also, $N_g=(4\omega\beta\alpha_m)^{1/2}$ is a normalization constant which scales the power in the surface polariton for unit width in the y direction to be equal to $|a_g|^2$. The tangential components of the electric fields in vacuum and the metal are obtained using, respectively, Eqs. (9) and (18) with $s=1$. The application of the boundary conditions as given by Eqs. (23a) and (23b) yields the dispersion relation

$$\beta=[\omega^2(1-\omega^2)/(1-2\omega^2)]^{1/2} . \tag{30}$$

Therefore, the surface polariton only exists in the frequency range $0<\omega<1/\sqrt{2}$. All the fields associated with the linear surface polariton are given in Appendix B.

B. Reradiation of the surface polariton

The surface polariton, on interaction with the small-amplitude grating, generates two Floquet modes which are of order $O(\delta^2)$. One of the Floquet modes is of the radiative type, whose phase is matched with the incident and the reflected quasi-plane-waves. This phase matching enables the incident quasi-plane-wave to transfer energy to the surface polariton. The $O(\delta^2)$ magnetic flux densities in vacuum and the metal, B_{y2}^{v} and B_{y2}^{m}, are determined from Eqs. (16) and (19) with $s=2$ and the first-order surface polariton fields as

$$\begin{aligned} B_{y2}^{v}=&\left[-\frac{\partial}{\partial x_1}+\frac{i\beta}{\alpha_v}\frac{\partial}{\partial z_1}+\frac{i\omega}{\alpha_v}\frac{\partial}{\partial t_1}\right]N_g a_g x_0\exp(-\alpha_v x_0)\exp[i(\beta z_0-\omega t_0)]\\ &+[a_i\exp(-ik_{v1}x_0)+b_r\exp(ik_{v1}x_0)]N_f\exp\{i[(\beta-K)z_0-\omega t_0]\}\\ &+f_1\exp(-\alpha_{v2}x_0)\exp\{i[(\beta+K)z_0-\omega t_0]\}+f_2\exp(-2\alpha_v x_0)\exp[i2(\beta z_0-\omega t_0)]+\text{c.c.} \end{aligned} \tag{31}$$

and

$$\begin{aligned} B_{y2}^{m}=&\left[-\frac{\partial}{\partial x_1}-\frac{i\beta}{\alpha_m}\frac{\partial}{\partial z_1}-\frac{i\omega}{\alpha_m}\frac{\partial}{\partial t_1}\right]N_g a_g x_0\exp(\alpha_m x_0)\exp[i(\beta z_0-\omega t_0)]\\ &+g_1\exp(\alpha_{m1}x_0)\exp\{i[(\beta-K)z_0-\omega t_0]\}\\ &+g_2\exp(\alpha_{m2}x_0)\exp\{i[(\beta+K)z_0-\omega t_0]\}+g_3\exp(\alpha_{2m}x_0)\exp[i2(\beta z_0-\omega t_0)]+\text{c.c.} , \end{aligned} \tag{32}$$

where

$$k_{v1}=[\omega^2-(\beta-K)^2]^{1/2} , \tag{33a}$$

$$\alpha_{v2}=[(\beta+K)^2-\omega^2]^{1/2} , \tag{33b}$$

and

$$\alpha_{m1}=[(\beta-K)^2-\omega^2+1]^{1/2} , \tag{34a}$$

$$\alpha_{m2}=[(\beta+K)^2-\omega^2+1]^{1/2} , \tag{34b}$$

$$\alpha_{2m}=(4\beta^2-4\omega^2+1)^{1/2} , \tag{34c}$$

where f_1, f_2, g_1, g_2, and g_3 are the amplitudes of the new wave components generated by the nonlinearity and the surface corrugation. The normalization constant N_f is chosen as $N_f=(2\omega/k_{v1})^{1/2}$ such that $-|a_i|^2$ and $|b_r|^2$ are the x component of the Poynting vector of the incident and the reflected waves, respectively.

The tangential components of the electric fields in vacuum and in the metal, E_{z2}^{v} and E_{z2}^{m}, are determined using, respectively, Eqs. (9) and (18) with $s=2$. The $O(\delta^2)$ boundary conditions given by Eqs. (24a) and (24b) are used to obtain the transport equation of the surface-polariton amplitude and the amplitudes of the newly generated wave components. The terms in the boundary conditions having the phase factor $\exp[i(\beta z_0-\omega t_0)]$ lead to

$$\left[\frac{\partial}{\partial t_1}+V_g\frac{\partial}{\partial z_1}\right]a_g=0 , \tag{35}$$

where $V_g=\partial\omega/\partial\beta$ is the group velocity of the linear surface polariton. The terms in the boundary condition having the second-harmonic phase factor $\exp[i2(\beta z_0-\omega t_0)]$ enable us to obtain

$$f_2=g_3=\tilde{f}_2 a_g^2=\tilde{g}_3 a_g^2=\frac{\omega\beta N_g^2 a_g^2}{(\omega^2-1)[\alpha_v(4\omega^2-1)+2\omega^2\alpha_{2m}]} . \tag{36}$$

The terms having the phase factor $\exp\{i[(\beta+K)z_0-\omega t_0]\}$ in the boundary condition yield

$$g_2=\tilde{g}_2 a_g=\eta N_g a_g \frac{(\alpha_v^2+K\beta-\alpha_m\alpha_{v2}-\alpha_v\alpha_{v2})(\omega^2-1)-\omega^2(\alpha_m^2+K\beta)}{2[(\omega^2-1)\alpha_{v2}+\omega^2\alpha_{m2}]} \tag{37a}$$

and

$$f_1=\tilde{f}_1 a_g=\eta N_g a_g \frac{(\alpha_v^2+K\beta)(\omega^2-1)+(\alpha_{m2}\alpha_m-\alpha_m^2-K\beta+\alpha_{m2}\alpha_v)\omega^2}{2[(\omega^2-1)\alpha_{v2}+\omega^2\alpha_{m2}]} . \tag{37b}$$

Lastly, the terms in the boundary conditions having the phase factor $\exp\{i[(\beta-K)z_0-\omega t_0]\}$ yield the result

$$b_r=C_{rr}a_i+C_{rg}a_g \tag{38a}$$

with

$$C_{rr}=\frac{\omega^2\alpha_{m1}+i(\omega^2-1)k_{v1}}{-\omega^2\alpha_{m1}+i(\omega^2-1)k_{v1}} , \tag{38b}$$

$$C_{rg}=\frac{\eta N_g[\omega^2(\alpha_m^2-\alpha_{m1}\alpha_v-\alpha_m\alpha_{m1}-K\beta)+(\omega^2-1)(K\beta-\alpha_v^2)]}{2N_f[-\omega^2\alpha_{m1}+i(\omega^2-1)k_{v1}]} , \tag{38c}$$

and

$$g_1=\frac{i2(\omega^2-1)k_{v1}N_f a_i}{-\omega^2\alpha_{m1}+i(\omega^2-1)k_{v1}}+\tilde{g}_1 a_g , \tag{39a}$$

where

$$\tilde{g}_1=\eta N_g \frac{\alpha_v(\alpha_m^2-K\beta)+\alpha_m(\alpha_v^2-K\beta)+i\alpha_m k_{v1}(\alpha_m+\alpha_v)}{-2(\alpha_v\alpha_{m1}+i\alpha_m k_{v1})} . \tag{39b}$$

Equation (38a) shows that the amplitude of the reflected wave b_r has a contribution from the incident-wave amplitude a_i and the amplitude of the surface polariton a_g. The parameter C_{rg} characterizes the strength of the reradiation of the surface polariton into the vacuum. Other second-order fields in vacuum and the metal are given in Appendix C. The incident quasi-plane-wave excites the surface polariton, which in turn produces second-harmonic fields. However, as is evident from the expressions of the second-order fields in vacuum (Appendix C), the order $O(\delta^2)$ part of the second-harmonic field is evanescent. The evanescent second-harmonic fields become radiative on interaction with the surface corrugation in $O(\delta^3)$.

C. Self-phase modulation and excitation

The self-phase modulation of and the incident wave coupling to the surface polariton take place in $O(\delta^3)$. The magnetic flux density fields in vacuum and the metal in $O(\delta^3)$, B_{y3}^v and B_{y3}^m, are evaluated from Eqs. (16) and (19) with $s=3$ and the first-order and second-order fields given in Appendixes B and C. Due to the nonlinear wave mixing and the scattering by the surface corrugation, B_{y3}^v and B_{y3}^m and the rest of the third-order fields contain a variety of components with the fundamental, second-harmonic, third-harmonic, as well as many Floquet-mode phase factors. The field components relevant to the present treatment are given in Appendix D. The terms with the phase factor $\exp[i(\beta z_0-\omega t_0)]$ in the third-order boundary conditions as given by Eqs. (25a) and (25b) lead to the following equation governing the self-phase modulation and the excitation of the surface polariton:

$$i\left[\frac{\partial}{\partial t_2}a_g+V_g\left[\frac{\partial}{\partial z_2}a_g+C_g a_g+C_{gr}a_i\right]\right]+P\frac{\partial^2}{\partial z_1^2}a_g=Q|a_g|^2 a_g , \tag{40}$$

where

$$\begin{aligned}C_g=&\frac{i\eta\omega^2\beta\alpha_m}{4(\omega^2-1)N_g}[2(\alpha_{m1}^2\tilde{g}_1+\alpha_{m2}^2\tilde{g}_2)+\eta\alpha_{mm}^3N_g+2K(\beta-K)\tilde{g}_1-2K(\beta+K)\tilde{g}_2]\\&+\frac{i\eta\beta\alpha_m}{4N_g}[-2\alpha_{v2}^2\tilde{f}_1+\eta\alpha_v^3N_g+2K(\beta+K)\tilde{f}_1]\\&-\frac{\eta^2\beta\alpha_m\{i(1-2\omega^2)^{1/2}[k_{v1}^2-K(\beta-K)]+\omega^2k_{v1}\}}{4(1-2\omega^2)^{1/2}[-\omega^2\alpha_{m1}+i(\omega^2-1)k_{v1}]}[\omega^2(\alpha_{m1}\alpha_v+\alpha_m\alpha_{m1}+K\beta-\alpha_m^2)+(\omega^2-1)(\alpha_v^2-K\beta)]\\&+\frac{i\eta\omega^2\beta\alpha_m}{4(1-2\omega^2)^{1/2}N_g}[2(\alpha_{m1}\tilde{g}_1+\alpha_{m2}\tilde{g}_2)+\eta\alpha_m^2N_g+2\alpha_{v2}\tilde{f}_1-\eta\alpha_v^2N_g] ,\end{aligned} \tag{41a}$$

$$C_{gr}=-\frac{\eta k_{v1}\beta\alpha_m N_f[\omega^2(\alpha_m^2-\alpha_{m1}\alpha_v-\alpha_m\alpha_{m1}-K\beta)+(\omega^2-1)(K\beta-\alpha_v^2)]}{N_g[-\omega^2\alpha_{m1}+i(\omega^2-1)k_{v1}]}\ , \tag{41b}$$

$$Q=-\frac{N_g^2\omega^3}{(1-2\omega^2)(2\omega^4-2\omega^2+1)}\left[\frac{\gamma(4\omega^4-4\omega^2+3)}{8(1-\omega^2)}+\frac{12\omega^4-12\omega^2+1}{2(4\omega^2-1)}+\frac{(1-\omega^2)[2\omega^2+(4\omega^4-2\omega^2+1)^{1/2}]}{(4\omega^2-1)[(4\omega^2-1)+2(4\omega^4-2\omega^2+1)^{1/2}]}\right]. \tag{41c}$$

The coefficient of self-phase modulation Q is given in Eq. (41c), where the term containing $\gamma(=1)$ gives the relativistic contribution to the self-phase modulation.[11] Also $P=\frac{1}{2}d^2\omega/d\beta^2$ is the coefficient of group velocity dispersion. The parameter C_{gr} characterizes the strength of the energy transfer from the incident radiative wave to the surface polariton. So far, the effect of losses in the metal have not been included. We assume that ν is the normalized collision frequency of the metal, then Eq. (40) is modified to[15]

$$i\left[\frac{\partial}{\partial t_2}a_g+V_g\left[\frac{\partial}{\partial z_2}a_g+(C_g+\alpha_g)a_g+C_{gr}a_i\right]\right]+P\frac{\partial^2}{\partial z_1^2}a_g=Q|a_g|^2a_g\ , \tag{42}$$

where $\alpha_g=\nu\omega\beta/[2(1-\omega^2)(1-2\omega^2)]$ is the loss coefficient.

The evolution of the amplitude of the surface polariton is governed by Eqs. (38a) and (40) or (42). With these results, we are now in a position to determine the amplitudes of the second-harmonic radiative waves.

V. SECOND-HARMONIC RADIATION

A. Second-harmonic radiation in −1 diffraction order

The strongest second-harmonic radiation fields are of the order $O(\delta^3)$, which has the phase dependence $\exp\{i[(2\beta-K)z_0-2\omega t_0]\}$, if the grating wave number is chosen suitably. Following the usual convention, we designate this second-harmonic radiation in -1 diffraction order. The bulk contribution comes from the nonlinear mixing of the first-order fields having the phase dependence $\exp[i(\beta z_0-\omega t_0)]$ and the second-order fields having the phase dependence $\exp\{i[(\beta-K)z_0-\omega t_0]\}$. The second-harmonic fields generated in the second order $O(\delta^2)$ have the phase dependence $\exp[i2(\beta z_0-\omega t_0)]$, which is evanescent. These fields, after being scattered by the surface corrugation, also have the phase dependence $\exp\{i([2\beta-K)z_0-2\omega t_0]\}$, constituting the surface contribution to the second-harmonic radiation in the -1 diffraction order. The magnetic flux density and the z component of the electric field associated with this radiative second-harmonic wave are expressed as

$$B^v_{y3,-1}=N_{f-1}A^v_{3,-1}\exp(ik_{v2}x_0)\exp\{i[(2\beta-K)z_0-2\omega t_0]\}+\text{c.c.}\ , \tag{43}$$

$$E^v_{z3,-1}=-\frac{k_{v2}}{2\omega}N_{f-1}A^v_{3,-1}\exp(ik_{v2}x_0)\exp\{i[(2\beta-K)z_0-2\omega t_0]\}+\text{c.c.}\ , \tag{44}$$

and

$$B^m_{y3,-1}=A^m_{3,-1}\exp(\alpha_{2m-}x_0)\exp\{i[(2\beta-K)z_0-2\omega t_0]\}+\text{c.c.}\ , \tag{45}$$

$$E^m_{z3,-1}=-\frac{i(2\beta-K)[\beta(\beta-K)-\alpha_m\alpha_{m1}]}{(4\omega^2-1)(\omega^2-1)^2}g_1N_ga_g\exp[(\alpha_m+\alpha_{m1})x_0]\exp\{i[(2\beta-K)z_0-2\omega_{t_0}]\}+\frac{i2\omega\alpha_{2m-}}{(4\omega^2-1)}A^m_{3,-1}\exp(\alpha_{2m-}x_0)\exp\{i[(2\beta-K)z_0-2\omega t_0]\}+\text{c.c.}\ , \tag{46}$$

where

$$k_{v2}=[4\omega^2-(2\beta-K)^2]^{1/2}\ , \tag{47a}$$

$$\alpha_{m2-}=[(2\beta-K)^2-4\omega^2+1]^{1/2}\ . \tag{47b}$$

The normalization constant is chosen as $N_{f-1}=(4\omega/k_{v2})^{1/2}$ so that $|A_{3,-1}|^2$ is the x component of the Poynting vector of the second-harmonic radiation in the -1 diffraction order. The $O(\delta^3)$ boundary conditions given by Eqs. (25a) and (25b) provide the relation between the amplitude of the second-harmonic radiation in the -1 diffraction order $[A^v_{3,-1},A^m_{3,-1}]$ and (a_i,a_g) through the terms having the phase factor $\exp\{i[(2\beta-K)z_0-2\omega t_0]\}$,

$$A^m_{3,-1}+\tfrac{1}{2}\eta\alpha_{2m}g_3a_g=N_{f-1}A^v_{3,-1}-\eta\alpha_v f_2 a_g\ , \tag{48}$$

$$-\frac{i2\omega\alpha_{2m-}}{(4\omega^2-1)}A^m_{3,-1}-\frac{i(2\beta-K)[\beta(\beta-K)-\alpha_m\alpha_{m1}]}{(4\omega^2-1)(\omega^2-1)^2}g_1N_ga_g-\frac{i\eta(2\beta-K)\alpha_mN_g^2a_g^2}{2(\omega^2-1)(4\omega^2-1)}+\frac{i\eta\omega(\alpha_{2m}^2-2K\beta)g_3}{4\omega^2-1}$$
$$=-\frac{k_{v2}}{2\omega}N_{f-1}A^v_{3,-1}+\frac{i\eta(2\alpha_v^2-K\beta)f_2a_g}{2\omega}\ . \tag{49}$$

From Eqs. (48) and (49) we determine the amplitude of the second-harmonic radiation in vacuum in the -1 diffraction order as

$$A^v_{3,-1}=\frac{2\omega(4\omega^2-1)}{[4\omega^2\alpha_{2m-}-i(4\omega^2-1)k_{v2}]N_{f-1}}$$
$$\times\Bigg[\frac{1}{2(4\omega^2-1)(\omega^2-1)^2}\{2\omega(\omega^2-1)^2\alpha_{2m-}\eta(\alpha_{2m+}2\alpha_v)g_3+2(2\beta-K)[\beta(\beta-K)-\alpha_m\alpha_{m1}]g_1N_ga_g$$
$$+(\omega^2-1)\eta\alpha_m(2\beta-K)N_g^2a_g^2-2\omega\eta(\omega^2-1)^2(\alpha_{2m}^2-2K\beta)g_3\}+\eta(2\alpha_v^2-K\beta)g_3/\omega\Bigg]\ . \tag{50}$$

This second-harmonic radiation in the -1 diffraction order is the strongest second-harmonic radiation.

B. Second-harmonic radiation in the specular direction

The second-harmonic radiation fields in the specular direction is of the $O(\delta^4)$ with the phase dependence $\exp\{i2[(\beta-K)z_0-\omega t_0]\}$. It is also the next strongest second-harmonic radiation. The bulk contribution to this radiation field comes from the nonlinear mixing of the first-order fields having the phase dependence $\exp[i(\beta z_0-\omega t_0)]$ with the third-order fields having the phase factor $\exp\{i[(\beta-2K)z_0-\omega t_0]\}$, and the wave mixing among the second-order fields having the phase dependence $\exp\{i[(\beta-K)z_0-\omega t_0]\}$. The surface contribution comes from the scattering of the third-order fields having the phase factor $\exp\{i[(2\beta-K)z_0-2\omega t_0]\}$. The magnetic flux density and the z component of the electric field having the phase factor $\exp\{i2[(\beta-K)z_0-\omega t_0]\}$ are determined from Eqs. (16) and (18) with $s=4$ to have the following form:

$$B^v_{y4}=N_fA^v_{4,s}\exp(i2k_{v1}x_0)\exp\{i2[(\beta-K)z_0-\omega t_0]\}+\text{c.c.}, \tag{51}$$

$$E^v_{z4}=-\frac{k_{v1}}{\omega}N_fA^v_{4,s}\exp(i2k_{v1}x_0)\exp\{i2[(\beta-K)z_0-\omega t_0]\}+\text{c.c.}, \tag{52}$$

and

$$B^m_{y4}=-\frac{[\alpha_m(\beta-2K)-\alpha_{m-2}\beta][4K(\beta-K)+\alpha_{m-2}^2-\alpha_m^2]}{2\omega(\omega^2-1)^2[(\alpha_m+\alpha_{m-2})^2-4(\beta-K)^2+4\omega^2-1]}N_ga_gA^m_{3,2}\exp[(\alpha_m+\alpha_{m-2})x_0]\exp\{i2[(\beta-K)z_0-\omega t_0]\}$$
$$+A^m_{4,s}\exp(\alpha_{2m-2}x_0)\exp\{i2[(\beta-K)z_0-\omega t_0]\}+\text{c.c.}, \tag{53}$$

$$E^m_{z4}=\Bigg[\Bigg[\frac{i[\alpha_m(\beta-2K)-\alpha_{m-2}\beta][(\alpha_{m-2}^2-\alpha_m^2)(\alpha_m+\alpha_{m-2})-\alpha_{2m-2}^2(\alpha_{m-2}-\alpha_m)]}{(\omega^2-1)^2[(\alpha_m+\alpha_{m-2})^2-\alpha_{2m-2}^2]}$$
$$-\frac{2i(\beta-K)}{(4\omega^2-1)(\omega^2-1)}\Bigg]N_ga_gA^m_{3,2}\exp[(\alpha_m+\alpha_{m-2})x_0]$$
$$-\frac{i(\beta-K)}{(4\omega^2-1)(\omega^2-1)}g_1^2\exp(2\alpha_{m1}x_0)+\frac{i2\omega\alpha_{2m-2}}{4\omega^2-1}A^m_{4,s}\exp(\alpha_{2m-2}x_0)\Bigg]\exp\{i2[(\beta-K)z_0-\omega t_0]\}+\text{c.c.} \tag{54}$$

in the vacuum and metal, respectively, where $A^m_{3,2}$ is given in Appendix D, and

$$\alpha_{m2-2}=[4(\beta-K)^2-4\omega^2+1]^{1/2}\ . \tag{55}$$

The normalization constant is chosen as N_f so that $|A_{4,s}|^2$ is the x component of the Poynting vector of the second-harmonic radiation in the specular direction. The $O(\delta^4)$ boundary conditions given by Eqs. (26a) and (26b) provide the relation between the amplitude of the second-harmonic radiation in the specular direction $[A^v_4, A^m_4]$ and (a_i, a_g)

through the terms having the phase factor $\exp\{i2[(\beta-K)z_0-\omega t_0]\}$:

$$-\frac{[\alpha_m(\beta-2K)-\alpha_{m-2}\beta][4K(\beta-K)+\alpha_{m-2}^2-\alpha_m^2]}{2\omega(\omega^2-1)^2[(\alpha_m+\alpha_{m-2})^2-\alpha_{2m-2}^2]}A_{3,2}^m N_g a_g+A_{4,s}^m+\frac{\eta\alpha_{2m-}}{2}A_{3,-1}^m+\frac{\eta^2\alpha_{2m}^2}{8}g_3$$
$$=N_f A_{4,s}^v+\frac{i\eta k_{v2}}{2}A_{3,-1}^v+\frac{\eta^2\alpha_v^2}{2}f_2\ , \quad (56)$$

$$\frac{i[\alpha_m(\beta-2K)-\alpha_{m-2}\beta]}{(4\omega^2-1)(\omega^2-1)^2}A_{3,2}^m N_g a_g\left[(\alpha_{m-2}-\alpha_m)-(\alpha_m+\alpha_{m-2})\frac{4K(\beta-K)+\alpha_{m-2}^2-\alpha_m^2}{(\alpha_m+\alpha_{m-2})^2-\alpha_{2m-2}^2}\right]$$
$$-\frac{i2(\beta-K)N_g a_g}{(4\omega^2-1)(\omega^2-1)}A_{3,2}^m-\frac{i(\beta-K)}{(4\omega^2-1)(\omega^2-1)}g_1^2+\frac{i2\omega\alpha_{2m-2}}{4\omega^2-1}A_{4,s}^m$$
$$+\frac{i\eta\omega[\alpha_{2m-}^2-K(2\beta-K)]}{4\omega^2-1}A_{3,-1}^m+\frac{i\eta(\alpha_m+\alpha_{m1})(2\beta-K)[\alpha_m\alpha_{m1}-\beta(\beta-K)]}{2(4\omega^2-1)(\omega^2-1)^2}N_g a_g g_1$$
$$+i\eta K\frac{[\alpha_m(\beta-K)-\alpha_{m1}\beta]K+(\omega^2-1)(\alpha_m+\alpha_{m1})}{2(4\omega^2-1)(\omega^2-1)^2}N_g a_g g_1$$
$$+\frac{i\eta^2\alpha_m^2(K-\beta)}{2(4\omega^2-1)(\omega^2-1)}N_g^2 a_g^2+\frac{i\eta^2\omega\alpha_{2m}(\alpha_{2m}^2-K\beta)}{4\omega^2-1}g_3$$
$$=-\frac{k_{v1}}{\omega}A_{v,s}^4-\frac{i\eta[k_{v2}^2+K(2\beta-K)]}{4\omega}A_{3,-1}^v+\frac{i\eta^2\alpha_v(K\beta-\alpha_v^2)}{2\omega}f_2\ . \quad (57)$$

From Eqs. (56) and (57) we determine the amplitude of the second-harmonic radiation in vacuum in the specular direction as

$$A_{4,s}^v=-\frac{i\eta}{4D}\{i4\omega^2\alpha_{2m-2}k_{v2}+(4\omega^2-1)[k_{v2}^2+K(2\beta-K)]\}A_{3,-1}^v$$
$$-\frac{i\eta^2\alpha_v}{2D}[2\omega^2\alpha_{2m-2}\alpha_v+(4\omega^2-1)(\alpha_v^2-K\beta)]f_2-\frac{i\eta\omega^2}{D}[\alpha_{2m-}(\alpha_{2m-}-\alpha_{2m-2})-K(2\beta-K)]A_{3,-1}^m$$
$$-\frac{i\eta^2\omega^2\alpha_{2m}}{4D}[\alpha_{2m}(\alpha_{2m}-\alpha_{2m-2})-4K\beta]g_3+\frac{i(\beta-K)\omega}{(\omega^2-1)D}g_1^2+\frac{i\eta^2\alpha_m^2\omega(K-\beta)}{2(\omega^2-1)D}N_g^2a_g^2$$
$$+\frac{i\omega}{(\omega^2-1)^2D}\left[(\alpha_{m-2}-\alpha_m)[\alpha_m(\beta-2K)-\alpha_{m-2}\beta]-2(\omega^2-1)(\beta-K)\right.$$
$$\left.-\frac{\alpha_m[\alpha_m(\beta-2K)-\alpha_{m-2}\beta][4K(\beta-K)+\alpha_{m-2}^2-\alpha_m^2]}{(\alpha_m+\alpha_{m-2})^2-\alpha_{2m-2}^2}\right]N_g a_g A_{3,2}^m$$
$$+\frac{i\omega\eta}{2(\omega^2-1)^2D}\{(\alpha_m+\alpha_{m1})(2\beta-K)[\alpha_m\alpha_{m1}-\beta(\beta-K)]$$
$$+K^2[\alpha_m(\beta-K)-\alpha_{m1}\beta]+(\omega^2-1)K(\alpha_m+\alpha_{m1})]\}N_g a_g g_1\ , \quad (58)$$

where

$$D=[k_{v1}(4\omega^2-1)+i2\omega^2\alpha_{2m-2}]N_f\ . \quad (59)$$

There exists also second-harmonic radiation fields in the +1 diffraction order, which are of the order $O(\delta^5)$. Since this second-harmonic radiation is considerably weaker than that in the −1 diffraction order, it is not included here.

VI. NUMERICAL RESULTS

Given the amplitude of incident fundamental fields $a_i(z,t)$, the amplitudes of the second-harmonic radiation mediated by the surface polariton in the −1 diffraction order, $A_{3,-1}^v$, and in the specular direction, A_{4s}^v, are completely determined by Eqs. (50), (57), and (58), with the help of Eqs. (38), (40), and (41) which govern the evolution of the surface-polariton amplitude. Illustrative numerical results of the enhancement factor and the beam properties of the second-harmonic radiation in the steady state ($\partial/\partial t=0$) are presented in this section.

A. Enhancement factor

We assume that the incident wave is a quasi-plane-wave of the form

$$N_f a_i \exp(ik_{v1}x_0)\exp\{i[(\beta-K)z_0-\omega t_0]\}\ .$$

The quasi-plane-wave has a finite transverse extent which intersects the z axis from $z=0$ to $z=L$. The second-harmonic reflection from a planar metal-vacuum interface is determined as

$$B_{y2}^{v}=N_f B_{2v}\exp(i2k_{v1}x_0)\times\exp\{i2[(\beta-K)z_0-\omega t_0]\}+\text{c.c.}, \quad (60\text{a})$$

where

$$B_{2v}=\frac{iN_f(\beta-K)\omega\cos^2\phi\exp(i2\phi)}{(1-\omega^2)[k_{v1}(1-4\omega^2)-i2\omega\alpha_{2m-2}]}a_i^2 , \quad (60\text{b})$$

$$\phi=\tan^{-1}\left[\frac{\alpha_{m1}\omega}{k_{v1}(1-\omega^2)}\right] . \quad (60\text{c})$$

The normalization constant N_f is the same as for the incident wave so that $|B_{2v}|^2$ gives the x component of the Poynting vector for the second-harmonic radiation from a planar metal-vacuum interface. The enhancement factors are defined as

$$E_{-1}=\frac{\int_0^L|A_{3,-1}^{v}|^2dz}{\int_0^L|B_{2v}|^2dz} , \quad (61\text{a})$$

$$E_s=\frac{\int_0^L|A_{4,s}^{v}|^2dz}{\int_0^L|B_{2v}|^2dz} , \quad (61\text{b})$$

for the enhanced second-harmonic radiation in the -1 diffraction order and in the specular direction, respectively.

We evaluate the enhancement factors for a silver-vacuum interface. The plasma frequency ω_p and the collision frequency ν of silver in rad/s are 1.2545×10^{16} and 2.2734×10^{14}, respectively.[16] The amplitude η and the period $2\pi/K$ of the sinusoidal surface corrugation are 15 and $\frac{1}{2000}$ mm, respectively. We assume that the width of the incident beam L is the same as the extent of the grating and is equal to the value that maximizes the excitation of the linear surface polariton, that is, $L=1.2565/\text{Re}\{C_g\}$.[15] The wavelength of the incident He-Ne laser light is 632.8 nm. The incident wave amplitude is of the form

$$a_i=a_{i0}\exp(ihz) , \quad (62)$$

where the adjustable parameter $h\ll|\beta-K|$ is used to vary the incident angle θ_i as given by $\theta_i=\tan^{-1}[(\beta-K+h)/\omega]$. The enhancement factors E_{-1} and E_s are plotted as functions of the incident angle θ_i in Figs. 2 and 3, respectively, with the incident intensity as a parameter. Both the lossless (solid line) and the lossy (dashed line) cases are included. The resonant behavior of the enhancement factors clearly shows that when the surface polariton is excited the second-harmonic radiation intensifies. The losses in the metal reduce the enhancement factors without significant changes in the resonant behavior. The enhancement factors depend also on the intensity of the incident wave. The maximum enhancement factors decrease as the incident intensity increase. The optimum incident angles at which the maximum enhancement factors occur change with the change in the incident intensity. The intensity dependence of the maximum enhancement factors and the optimum incident angles are presented in Figs. 4 and 5 for the second-harmonic radiation in the -1 diffraction order, and in Figs. 6 and 7 for the second-harmonic radiation in the specular direction. When the incident intensity is

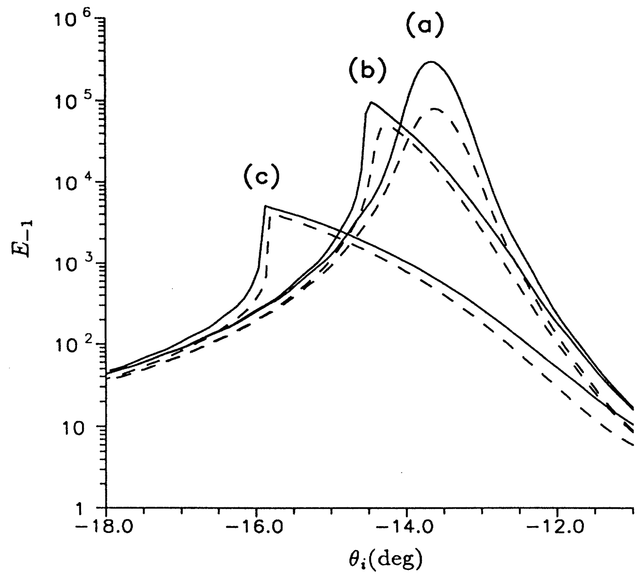

FIG. 2. Enhancement factor as a function of the angle of incidence for the second-harmonic radiation in the -1 diffraction order. Curves (a), (b), and (c) correspond to normalized incident intensities of 10^{-4}, 10^{-3}, and 10^{-2}, respectively. Solid lines are for the lossless case; dashed lines are for the lossy case.

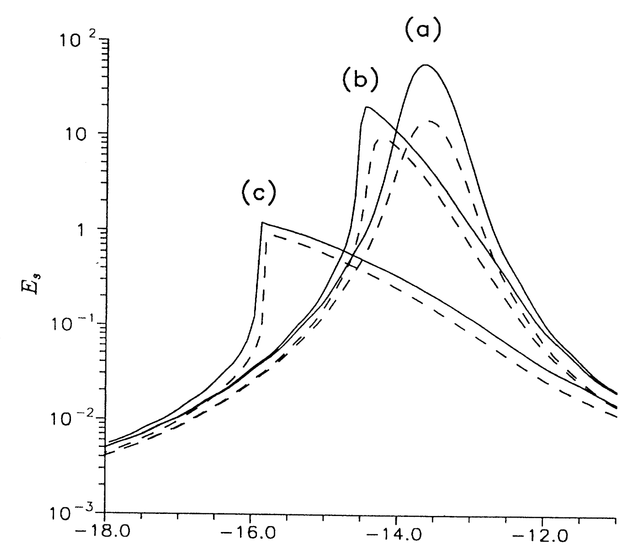

FIG. 3. Enhancement factor as a function of the incident angle for the second-harmonic radiation in the specular direction. Other parameters are the same as in Fig. 2.

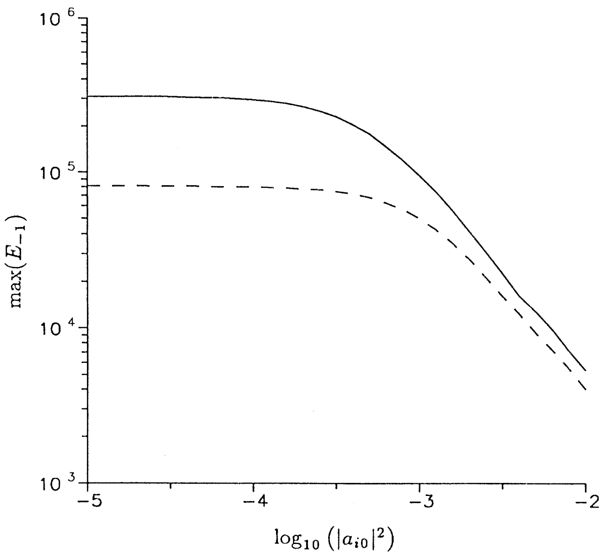

FIG. 4. The maximum enhancement factor as a function of the logarithm of the incident intensity for the second-harmonic radiation in the -1 diffraction order. Solid line is for the lossless case; dashed line is for the lossy case.

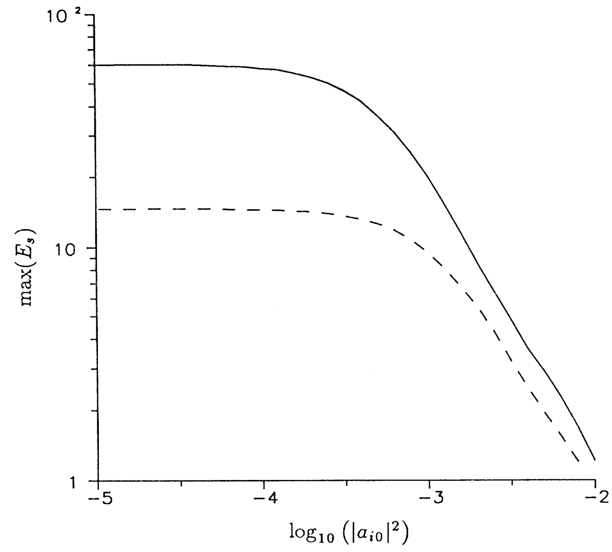

FIG. 6. Same as Fig. 4 for the second-harmonic radiation in the specular direction.

small, the nonlinear effects are very weak. The excitation of the surface polariton is very efficient as a result of the choice of the extent of the grating L. For the enhanced second-harmonic radiation in the -1 diffraction order, the enhancement factors in the linear limit are approximately 3×10^5 and 8×10^4 for the lossless and lossy cases, respectively. For the enhanced second-harmonic radiation in the specular direction, the enhancement factors in the linear limit are approximation 60.0 and 15.0 for the lossless and lossy cases, respectively. These results are in good qualitative agreement with the experimental result obtained by Quail and Simon.[13] The width of the resonance curve is larger than that obtained by Quail and Simon, where the incident wave is assumed to be a plane wave and the method of reduced Rayleigh equations was used. The maximum enhancement factors decrease sharply as the incident intensity exceeds a critical value of about 0.001 (normalized), accompanied by corresponding changes in the optimum incident angles.

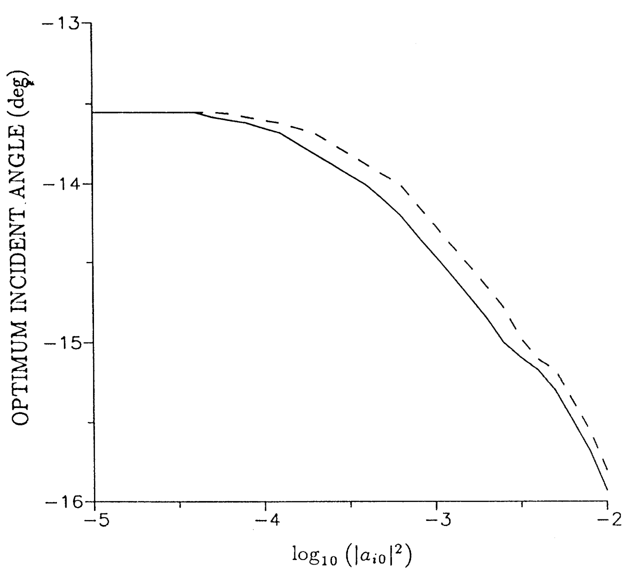

FIG. 5. The intensity dependence of the optimum incident angle at which the maximum enhancement factor for the second-harmonic radiation in the -1 diffraction order (Fig. 4) is achieved. Solid line is for the lossless case; dashed line is for the lossy case.

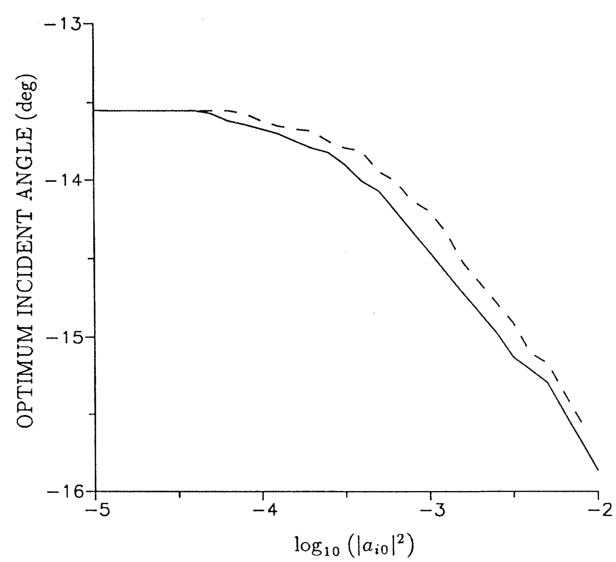

FIG. 7. Same as Fig. 5 for the second-harmonic radiation in the specular direction.

B. Beam properties

Next, we examine some of the beam properties of the enhanced second-harmonic radiation. The geometry for the surface-enhanced second-harmonic generation is the same as before except that the extent of the grating is now assumed to be infinite. The incident wave amplitude has a slowly varying Gaussian profile. The width [see Eq. (63)] of the Gaussian profile is L [optimum extent of the grating for the linear excitation of the surface polariton $L=2202.2$ (normalized) or $L=52.7$ μm (physical units)] so that a_i is now described by

$$a_i = a_{i0}\exp\left[\frac{-z^2}{(L/2)^2}\right]. \tag{63}$$

The profiles (normalized by the peak amplitude) of the enhanced second-harmonic radiation in the -1 diffraction order and in the specular direction are very similar. Hence only the results for the -1 diffraction order are presented. The normalized beam profiles of the second-harmonic radiation in the -1 diffraction order for both the lossless and lossy cases are shown in Figs. 8, 9, and 10 for peak intensities ($|a_{i0}|^2$) of 10^{-4}, 10^{-3}, and 10^{-2}, respectively. At low levels of incident intensity (Fig. 8, for example), the profile of the second-harmonic radiation remains approximately Gaussian with a slight broadening for the lossless case and a slight narrowing for the lossy case. The center of the beam profile is shifted in the direction of the propagation of the surface polariton. The amount of the shift is comparable to the width of the incident Gaussian profile. The lateral shift is more pronounced for the lossless case than for the lossy case at low incident intensities. The profile of the second-harmonic radiation progressively deviates from the Gaussian form as the incident intensity increases. At intermediate levels of the incident intensities (Fig. 9, for example), asymmetries in the beam profile develop with prolonged tails. The amount of the lateral shift decreases with increase in the incident intensity. The full width at half maximum (FWHM) of the profile also decreases with the increase in the incident intensity. At high levels of the incident intensities (Fig. 10, for example), the profile is quite different from the Gaussian shape. The peak amplitude in the second-harmonic radiation is reached (spatially) before the incident amplitude reaches its maximum. This is because at high incident intensity levels, the self-phase modulation of the surface polariton frustrates the phase-matching condition before the incident

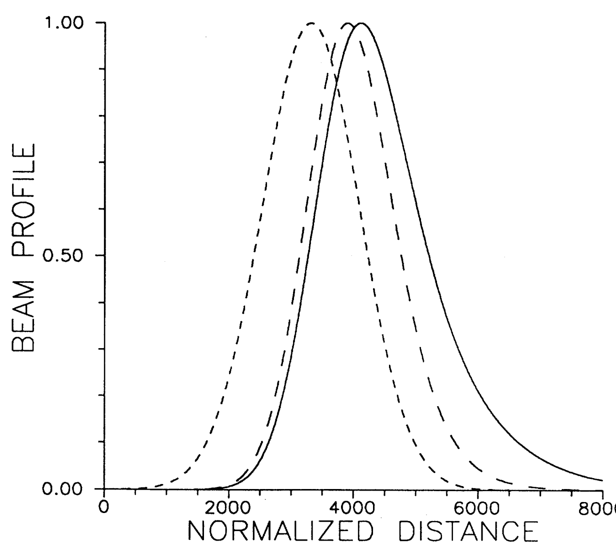

FIG. 8. Profile of the amplitude of the second-harmonic radiation in the -1 diffraction order when the incident wave has a Gaussian profile of width $L=2202.0$ (normalized) (short-dashed line). The peak incident intensity is 10^{-4}. The extent of the grating is assumed to be infinite. Solid line is for the lossless case; long-dashed line is for the lossy case.

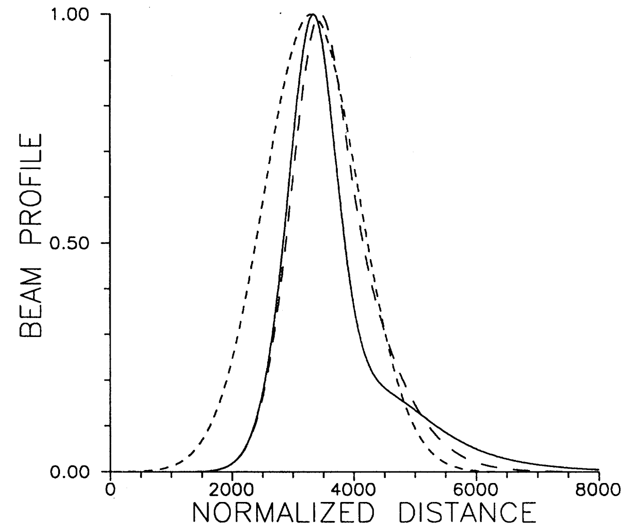

FIG. 9. Same as Fig. 8 for the peak intensity of 10^{-3}.

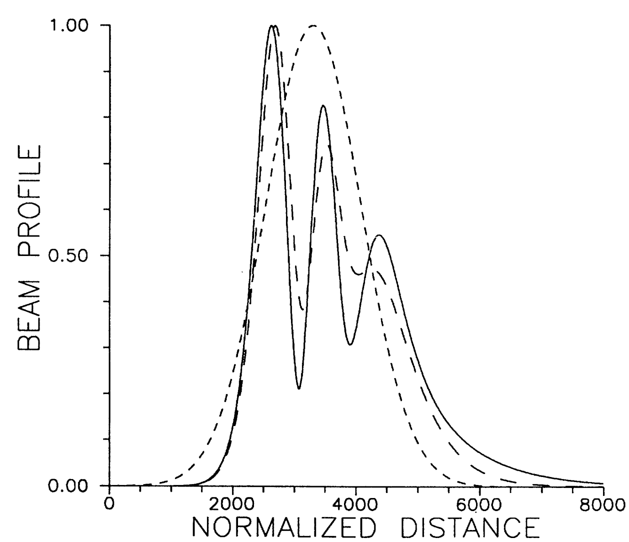

FIG. 10. Same as Fig. 8 for the peak intensity of 10^{-2}.

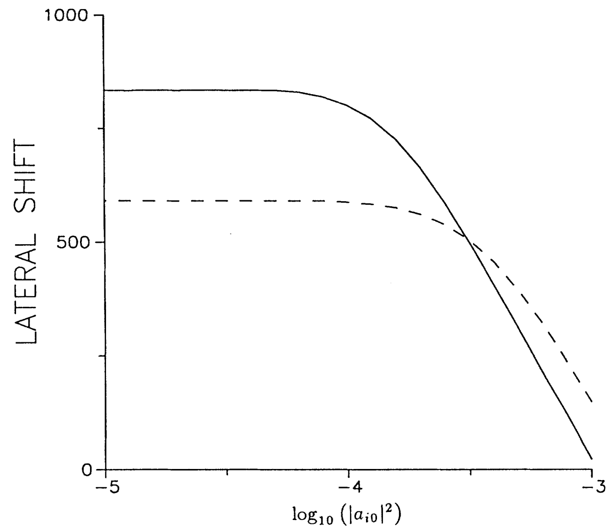

FIG. 11. The lateral shift of the beam profile of the second-harmonic radiation in the -1 diffraction order as a function of the peak intensity of the Gaussian profile of the incident beam of width $L=2202.0$ (normalized). Solid line is for the lossless case; dashed line is for the lossy case.

amplitude reaches its maximum. Thus, at the peak amplitude of the incident wave, the efficiency of excitation of the surface polariton is very low. For the range of the incident intensity for which the reflected second-harmonic radiation has approximately the Gaussian profile, we have plotted in Fig. 11 the lateral shift and in Fig. 12 the FWHM as functions of the peak incident intensity for

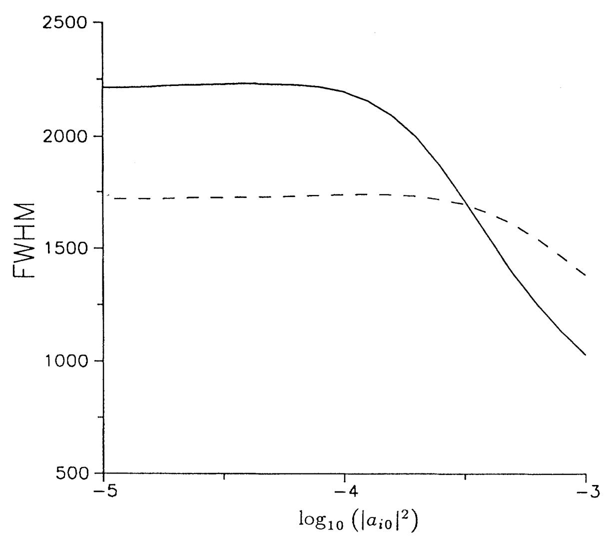

FIG. 12. The full width at half maximum of the profile of the second-harmonic radiation in the -1 diffraction order as a function of the peak intensity of the incident Gaussian beam of width $L=2202.0$ (normalized). Solid line is for the lossless case; dashed line is for the lossy case.

both the lossless and the lossy cases. At low intensity levels, the lateral shift for the lossless case is considerably larger than for the lossy case. There exists an intensity level at which the lateral shifts are the same for the lossless and the lossy cases. Beyond that intensity level the lateral shift for the lossy case is larger than that for the lossless case. Similar behavior in the FWHM is also observed as Fig. 12 shows.

VII. CONCLUDING REMARKS

Surface-enhanced second-harmonic generation is a nonlinear process. To study the spatiotemporal behavior (dynamics of beams) of this process, the method of decomposition of the incident pulsed beam into an integral of plane waves fails because the principle of superposition is invalid. Further complication arises due to the fact that (a) the amplitude of the surface polariton experiences self-phase modulation, and (b) the efficiency of excitation of the surface polariton depends on the incident intensity due to the nonlinearity in the metal. We have investigated the characteristics of the surface-enhanced second-harmonic generation of pulsed beams, using a singular perturbation procedure employing multiple space and time scales. For smooth pulsed beams, the slow variation of the wave amplitude is expressed by derivatives on long space and time scales (rather than integrals), enabling us to linearize the problem in each order of the perturbation. In so doing, the effects of the self-phase modulation and the nonlinear excitation of the surface polariton on the enhanced second-harmonic generation are successfully taken into account.

The resonant behavior of the enhancement factor with respect to the incident angle for an incident plane wave of infinite width has been presented previously.[2,4] Complementing those results, we have presented here the resonant behavior for an incident quasi-plane-wave of finite width. Moreover, the intensity dependence of the enhancement factor and the optimum incident angle for a quasi-plane-wave are included. These intensity dependences are expected for nonlinear processes. When the incident wave has a Gaussian profile, lateral shift of the second-harmonic radiation, which is the nonlinear counterpart of the well-known Goos-Haenchen shift, is predicted. This lateral shift is quite pronounced in the near-linear regime of the incident intensity and should be observable in experiments.

APPENDIX A: THE SOURCE TERMS

The following are source terms for the second-order fields:

$$S_{12}=\frac{\partial}{\partial t_1}B^v_{y1}+\frac{\partial}{\partial z_1}E^v_{x1}-\frac{\partial}{\partial x_1}E^v_{z1}\ , \tag{A1}$$

$$S_{22}=-\frac{\partial}{\partial t_1}E^v_{x1}-\frac{\partial}{\partial z_1}B^v_{y1}\ , \tag{A2}$$

$$S_{32}=-\frac{\partial}{\partial t_1}E^v_{z1}+\frac{\partial}{\partial x_1}B^v_{y1}\ , \tag{A3}$$

$$S_{42}=\frac{\partial}{\partial t_1}B^m_{y1}+\frac{\partial}{\partial z_1}E^m_{x1}-\frac{\partial}{\partial x_1}E^m_{z1}\ , \tag{A4}$$

$$S_{52}=-\frac{\partial}{\partial t_1}E^m_{x1}+N_1V_{x1}-\frac{\partial}{\partial z_1}B^m_{y1}\ , \tag{A5}$$

$$S_{62}=-\frac{\partial}{\partial t_1}E^m_{z1}+N_1V_{z1}+\frac{\partial}{\partial x_1}B^m_{y1}\ , \tag{A6}$$

$$S_{72}=-\frac{\partial}{\partial t_1}N_1-\frac{\partial}{\partial x_0}(N_1V_{x1})-\frac{\partial}{\partial x_1}V_{x1}-\frac{\partial}{\partial z_0}(N_1N_{z1})-\frac{\partial}{\partial z_1}V_{z1}\ , \tag{A7}$$

$$S_{82}=-\frac{\partial}{\partial t_1}V_{x1}-V_{x1}\frac{\partial}{\partial x_0}V_{x1}-V_{z1}\frac{\partial}{\partial z_0}V_{x1}+V_{z1}B^m_{y1}\ , \tag{A8}$$

$$S_{92}=-\frac{\partial}{\partial t_1}V_{z1}-V_{x1}\frac{\partial}{\partial x_0}V_{z1}-V_{z1}\frac{\partial}{\partial z_0}V_{z1}-V_{x1}B^m_{y1}\ . \tag{A9}$$

The following are source terms for the third-order fields:

$$S_{13}=\frac{\partial}{\partial t_1}B^v_{y2}+\frac{\partial}{\partial t_2}B^v_{y1}+\frac{\partial}{\partial z_1}E^v_{x2}+\frac{\partial}{\partial z_2}E^v_{x1}-\frac{\partial}{\partial x_1}E^v_{z2}-\frac{\partial}{\partial x_2}E^v_{z1}\ , \tag{A10}$$

$$S_{23}=-\frac{\partial}{\partial t_1}E^v_{x2}-\frac{\partial}{\partial t_2}E^v_{x1}-\frac{\partial}{\partial z_1}B^v_{y2}-\frac{\partial}{\partial z_2}B^v_{y1}\ , \tag{A11}$$

$$S_{33}=-\frac{\partial}{\partial t_1}E^v_{z2}-\frac{\partial}{\partial t_2}E^v_{z1}+\frac{\partial}{\partial x_1}B^v_{y2}+\frac{\partial}{\partial x_2}B^v_{y1}\ , \tag{A12}$$

$$S_{43}=\frac{\partial}{\partial t_1}B^m_{y2}+\frac{\partial}{\partial t_2}B^m_{y1}+\frac{\partial}{\partial z_1}E^m_{x2}+\frac{\partial}{\partial z_2}E^m_{x1}-\frac{\partial}{\partial x_1}E^m_{z2}-\frac{\partial}{\partial x_2}E^m_{z1}\ , \tag{A13}$$

$$S_{53}=-\frac{\partial}{\partial t_1}E^m_{x2}-\frac{\partial}{\partial t_2}E^m_{x1}+N_1V_{x2}+N_2V_{x1}-\frac{\partial}{\partial z_1}B^m_{y2}-\frac{\partial}{\partial z_2}B^m_{y1}\ , \tag{A14}$$

$$S_{63}=-\frac{\partial}{\partial t_1}E^m_{z2}-\frac{\partial}{\partial t_2}E^m_{z1}+N_1V_{z2}+N_2V_{z1}+\frac{\partial}{\partial x_1}B^m_{y2}+\frac{\partial}{\partial x_2}B^m_{y1}\ , \tag{A15}$$

$$S_{73}=-\frac{\partial}{\partial t_1}N_2-\frac{\partial}{\partial t_2}N_1-\frac{\partial}{\partial x_0}(N_2V_{x1}+N_1V_{x2})-\frac{\partial}{\partial z_0}(N_2V_{z1}+N_1V_{z2})-\frac{\partial}{\partial x_1}V_{x2}-\frac{\partial}{\partial x_2}V_{x1}-\frac{\partial}{\partial z_1}V_{z2}-\frac{\partial}{\partial z_2}V_{z1}-\frac{\partial}{\partial x_1}(N_1V_{x1})-\frac{\partial}{\partial z_1}(N_1V_{z1})\ , \tag{A16}$$

$$S_{83}=-\frac{\partial}{\partial t_1}V_{x2}-\frac{\partial}{\partial t_2}V_{x1}-V_{x1}\frac{\partial}{\partial x_0}V_{x2}-V_{x1}\frac{\partial}{\partial x_1}V_{x1}-V_{x2}\frac{\partial}{\partial x_0}V_{x1}-V_{z1}\frac{\partial}{\partial z_0}V_{x2}-V_{z1}\frac{\partial}{\partial z_1}V_{x1}-V_{z2}\frac{\partial}{\partial z_0}V_{x1}+V_{z1}B^m_{y2}+V_{z2}B^m_{y1}-\frac{1}{2}\frac{\partial}{\partial t_0}[(V^2_{x1}+V^2_{z1})V_{x1}]\ , \tag{A17}$$

$$S_{93}=-\frac{\partial}{\partial t_1}V_{z2}-\frac{\partial}{\partial t_2}V_{z1}-V_{z1}\frac{\partial}{\partial z_0}V_{z2}-V_{z1}\frac{\partial}{\partial z_1}V_{z1}-V_{z2}\frac{\partial}{\partial z_0}V_{z1}-V_{x1}\frac{\partial}{\partial x_0}V_{z2}-V_{x1}\frac{\partial}{\partial x_1}V_{z1}-V_{x2}\frac{\partial}{\partial x_0}V_{z1}-V_{x1}B^m_{y2}-V_{x2}B^m_{y1}-\frac{1}{2}\frac{\partial}{\partial t_0}[(V^2_{x1}+V^2_{z1})V_{z1}]\ . \tag{A18}$$

The following are source terms for the fourth-order fields:

$$S_{14}=\frac{\partial}{\partial t_1}B^v_{y3}+\frac{\partial}{\partial t_2}B^v_{y2}+\frac{\partial}{\partial t_3}B^v_{y1}+\frac{\partial}{\partial z_1}E^v_{x3}+\frac{\partial}{\partial z_2}E^v_{x2}+\frac{\partial}{\partial z_3}E^v_{x1}-\frac{\partial}{\partial x_1}E^v_{z3}-\frac{\partial}{\partial x_2}E^v_{x2}-\frac{\partial}{\partial x_3}E^v_{z1}\ , \tag{A19}$$

$$S_{24}=-\frac{\partial}{\partial t_1}E^v_{x3}-\frac{\partial}{\partial t_2}E^v_{x2}-\frac{\partial}{\partial t_3}E^v_{x1}-\frac{\partial}{\partial z_1}B^v_{y3}-\frac{\partial}{\partial z_2}B^v_{y2}-\frac{\partial}{\partial z_3}B^v_{y1}, \tag{A20}$$

$$S_{34}=-\frac{\partial}{\partial t_1}E^v_{z3}-\frac{\partial}{\partial t_2}E^v_{z2}-\frac{\partial}{\partial t_3}E^v_{z1}+\frac{\partial}{\partial x_1}B^v_{y3}+\frac{\partial}{\partial x_2}B^v_{y2}+\frac{\partial}{\partial x_3}B^v_{y1}\ , \tag{A21}$$

$$S_{44}=\frac{\partial}{\partial t_1}B^m_{y3}+\frac{\partial}{\partial t_2}B^m_{y2}+\frac{\partial}{\partial t_3}B^m_{y1}+\frac{\partial}{\partial z_1}E^m_{x3}+\frac{\partial}{\partial z_2}E^m_{x2}+\frac{\partial}{\partial z_3}E^m_{x1}-\frac{\partial}{\partial x_1}E^m_{z3}-\frac{\partial}{\partial x_2}E^m_{z2}-\frac{\partial}{\partial x_3}E^m_{z1}\ , \tag{A22}$$

$$S_{54}=-\frac{\partial}{\partial t_1}E^m_{x3}-\frac{\partial}{\partial t_2}E^m_{x2}-\frac{\partial}{\partial t_3}E^m_{x1}+N_1V_{x3}+N_2V_{x2}+N_3V_{x1}-\frac{\partial}{\partial z_1}B^m_{y3}-\frac{\partial}{\partial z_2}B^m_{y2}-\frac{\partial}{\partial z_3}B^m_{y1}\ , \tag{A23}$$

$$S_{64}=-\frac{\partial}{\partial t_1}E^m_{z3}-\frac{\partial}{\partial t_2}E^m_{z2}-\frac{\partial}{\partial t_3}E^m_{z1}+N_1V_{z3}+N_2V_{z2}+N_3V_{z1}+\frac{\partial}{\partial x_1}B^m_{y3}+\frac{\partial}{\partial x_2}B^m_{y2}+\frac{\partial}{\partial x_3}B^m_{y1}\ , \tag{A24}$$

$$S_{74} = -\frac{\partial}{\partial t_1}N_3 - \frac{\partial}{\partial t_2}N_2 - \frac{\partial}{\partial t_3}N_1 - \frac{\partial}{\partial x_0}(N_3V_{x1}+N_2V_{x2}+N_1V_{x3}) - \frac{\partial}{\partial x_1}(N_1V_{x2}+N_2V_{x1}+V_{x3})$$
$$-\frac{\partial}{\partial x_2}(N_1V_{x1}+V_{x2}) - \frac{\partial}{\partial x_3}V_{x1} - \frac{\partial}{\partial z_1}(N_1V_{z2}+N_2V_{z1}+V_{z3}) - \frac{\partial}{\partial z_2}(N_1V_{z1}+V_{z2}) - \frac{\partial}{\partial z_3}V_{z1}$$
$$-\frac{\partial}{\partial z_0}(N_3V_{z1}+N_2V_{z2}+N_1V_{z3}) \ , \tag{A25}$$

$$S_{84} = -\left[V_{x1}\frac{\partial}{\partial x_0} + V_{z1}\frac{\partial}{\partial z_0} + \frac{\partial}{\partial t_1}\right][V_{x3}+\tfrac{1}{2}(V_{x1}^2+V_{z1}^2)V_{x1}]$$
$$-\left[\frac{\partial}{\partial t_2} + V_{x1}\frac{\partial}{\partial x_1} + V_{x2}\frac{\partial}{\partial x_0} + V_{z1}\frac{\partial}{\partial z_1} + V_{z2}\frac{\partial}{\partial z_0}\right]V_{x2}$$
$$-\left[\frac{\partial}{\partial t_3} + V_{x1}\frac{\partial}{\partial x_2} + V_{x2}\frac{\partial}{\partial x_1} + V_{x3}\frac{\partial}{\partial x_0} + V_{z1}\frac{\partial}{\partial z_2} + V_{z2}\frac{\partial}{\partial z_1} + V_{z3}\frac{\partial}{\partial z_0}\right]V_{x1}$$
$$-\frac{\partial}{\partial t_0}[\tfrac{1}{2}(V_{x1}^2+V_{z1}^2)V_{x2} + (V_{x1}V_{x2}+V_{z1}V_{z2})V_{x1}] + V_{z1}B_{y3}^m + V_{z2}B_{y2}^m + V_{z3}B_{y1}^m \ , \tag{A26}$$

$$S_{94} = -\left[V_{x1}\frac{\partial}{\partial x_0} + V_{z1}\frac{\partial}{\partial z_0} + \frac{\partial}{\partial t_1}\right][V_{z3}+\tfrac{1}{2}(V_{x1}^2+V_{z1}^2)V_{z1}]$$
$$-\left[\frac{\partial}{\partial t_2} + V_{x1}\frac{\partial}{\partial x_1} + V_{x2}\frac{\partial}{\partial x_0} + V_{z1}\frac{\partial}{\partial z_1} + V_{z2}\frac{\partial}{\partial z_0}\right]V_{z2}$$
$$-\left[\frac{\partial}{\partial t_3} + V_{x1}\frac{\partial}{\partial x_2} + V_{x2}\frac{\partial}{\partial x_1} + V_{x3}\frac{\partial}{\partial x_0} + V_{z1}\frac{\partial}{\partial z_2} + V_{z2}\frac{\partial}{\partial z_1} + V_{z3}\frac{\partial}{\partial z_0}\right]V_{z1}$$
$$-\frac{\partial}{\partial t_0}[\tfrac{1}{2}(V_{x1}^2+V_{z1}^2)V_{z2} + (V_{x1}V_{x2}+V_{z1}V_{z2})V_{z1}] - V_{x1}B_{y3}^m - V_{x2}B_{y2}^m - V_{x3}B_{y1}^m \ . \tag{A27}$$

APPENDIX B: FIRST-ORDER FIELDS; THE SURFACE POLARITON

$$B_{y1}^v = N_g a_g \exp(-\alpha_v x_0)\exp[i(\beta z_0 - \omega t_0)] + \text{c.c.}, \ , \tag{B1}$$

$$E_{x1}^v = \frac{\beta}{\omega} N_g a_g \exp(-\alpha_v x_0)\exp[i(\beta z_0 - \omega t_0)] + \text{c.c.}, \tag{B2}$$

$$E_{z1}^v = -\frac{i\alpha_v}{\omega} N_g a_g \exp(-\alpha_v x_0)\exp[i(\beta z_0 - \omega t_0)] + \text{c.c.}, \tag{B3}$$

$$B_{y1}^m = N_g a_g \exp(\alpha_m x_0)\exp[i(\beta z_0 - \omega t_0)] + \text{c.c.}, \tag{B4}$$

$$E_{x1}^m = \frac{\omega\beta}{\omega^2-1} N_g a_g \exp(\alpha_m x_0)\exp[i(\beta z_0 - \omega t_0)] + \text{c.c.}, \tag{B5}$$

$$E_{z1}^m = \frac{i\omega\alpha_m}{\omega^2-1} N_g a_g \exp(\alpha_m x_0)\exp[i(\beta z_0 - \omega t_0)] + \text{c.c.}, \tag{B6}$$

$$V_{x1} = -\frac{i\beta}{\omega^2-1} N_g a_g \exp(\alpha_m x_0)\exp[i(\beta z_0 - \omega t_0)] + \text{c.c.}, \tag{B7}$$

$$V_{z1} = \frac{\alpha_m}{\omega^2-1} N_g a_g \exp(\alpha_m x_0)\exp[i(\beta z_0 - \omega t_0] + \text{c.c.}, \tag{B8}$$

$$N_1 = 0 \ . \tag{B9}$$

APPENDIX C: SECOND-ORDER FIELDS

$$B_{y2}^{v}=\left[-\frac{\partial}{\partial x_1}+\frac{i\beta}{\alpha_v}\frac{\partial}{\partial z_1}+\frac{i\omega}{\alpha_v}\frac{\partial}{\partial t_1}\right]N_g a_g x_0\exp(-\alpha_v x_0)\exp[i(\beta z_0-\omega t_0)]$$
$$+[a_i\exp(-ik_{v1}x_0)+b_r\exp(ik_{v1}x_0)]N_f\exp\{i[(\beta-K)z_0-\omega t_0]\}$$
$$+f_1\exp(-\alpha_{v2}x_0)\exp\{i[(\beta+K)z_0-\omega t_0]\}+f_2\exp(-2\alpha_v x_0)\exp[i2(\beta z_0-\omega t_0)]+\text{c.c.},\qquad\text{(C1)}$$

$$E_{x2}^{v}=\frac{i}{\omega}\left[i\beta x_0\frac{\partial}{\partial x_1}+\left[-1+\frac{\beta^2 x_0}{\alpha_v}\right]\frac{\partial}{\partial z_1}+\left[-\frac{\beta}{\omega}+\frac{\omega\beta x_0}{\alpha_v}\right]\frac{\partial}{\partial t_1}\right]N_g a_g\exp(-\alpha_v x_0)\exp[i(\beta z_0-\omega t_0)]$$
$$+\frac{\beta-K}{\omega}[a_i\exp(-ik_{v1}x_0)+b_r\exp(ik_{v1}x_0)]N_f\exp\{i[(\beta-K)z_0-\omega t_0]\}$$
$$+\frac{\beta+K}{\omega}f_1\exp(-\alpha_{v2}x_0)\exp\{i[(\beta+K)z_0-\omega t_0]\}+\frac{\beta}{\omega}f_2\exp(-2\alpha_v x_0)\exp[i2(\beta z_0-\omega t_0)]+\text{c.c.},\qquad\text{(C2)}$$

$$E_{z2}^{v}=\frac{i}{\omega}\left[\alpha_v x_0\frac{\partial}{\partial x_1}+\frac{i\beta}{\alpha_v}(1-\alpha_v x_0)\frac{\partial}{\partial z_1}+i\left[\frac{\beta^2}{\omega\alpha_v}-\omega x_0\right]\frac{\partial}{\partial t_1}\right]N_g a_g\exp(-\alpha_v x_0)\exp[i(\beta z_0-\omega t_0)]$$
$$+\frac{k_{v1}}{\omega}[a_i\exp(-ik_{v1}x_0)-b_r\exp(ik_{v1}x_0)]N_f\exp\{i[(\beta-K)z_0-\omega t_0]\}$$
$$-\frac{i\alpha_{v2}}{\omega}f_1\exp(-\alpha_{v2}x_0)\exp\{i[(\beta+K)z_0-\omega t_0]\}-\frac{i\alpha_v}{\omega}f_2\exp(-2\alpha_v x_0)\exp[i2(\beta z_0-\omega t_0)]+\text{c.c.},\qquad\text{(C3)}$$

$$B_{y2}^{m}=\left[-\frac{\partial}{\partial x_1}-\frac{i\beta}{\alpha_m}\frac{\partial}{\partial z_1}-\frac{i\omega}{\alpha_m}\frac{\partial}{\partial t_1}\right]N_g a_g x_0\exp(\alpha_m x_0)\exp[i(\beta z_0-\omega t_0)]+g_1\exp(\alpha_{m1}x_0)\exp\{i[(\beta-K)z_0-\omega t_0]\}$$
$$+g_2\exp(\alpha_{m2}x_0)\exp\{i[(\beta+K)z_0-\omega t_0]\}+g_3\exp(\alpha_{2m}x_0)\exp[i2(\beta z_0-\omega t_0)]+\text{c.c.},\qquad\text{(C4)}$$

$$E_{x2}^{m}=\left[-\frac{\omega\beta x_0}{\omega^2-1}\frac{\partial}{\partial x_1}-\frac{i\omega}{\omega^2-1}\left[1+\frac{\beta^2 x_0}{\alpha_m}\right]\frac{\partial}{\partial z_1}-\frac{i\beta}{\omega^2-1}\left[\frac{\omega^2+1}{\omega^2-1}+\frac{\omega^2 x_0}{\alpha_m}\right]\frac{\partial}{\partial t_1}\right]N_g a_g$$
$$\times\exp(\alpha_m x_0)\exp[i(\beta z_0-\omega t_0)]-\frac{\alpha_m N_g^2 a_g^2}{(\omega^2-1)(4\omega^2-1)}\exp(2\alpha_m x_0)\exp[i2(\beta z_0-\omega t_0)]$$
$$-\frac{\alpha_m N_g^2|a_g|^2}{(\omega^2-1)(2\omega^2-1)}\exp(2\alpha_m x_0)+\frac{\omega(\beta-K)}{\omega^2-1}g_1\exp(\alpha_{m1}x_0)\exp\{i[(\beta-K)z_0-\omega t_0]\}$$
$$+\frac{\omega(\beta+K)}{\omega^2-1}g_2\exp(\alpha_{m2}x_0)\exp\{i[(\beta+K)z_0-\omega t_0)\}+\frac{4\omega\beta}{4\omega^2-1}g_3\exp(\alpha_{2m}x_0)\exp[i2(\beta z_0-\omega t_0)]+\text{c.c.},\qquad\text{(C5)}$$

$$E_{z2}^{m}=\left[-\frac{i\omega\alpha_m x_0}{\omega^2-1}\frac{\partial}{\partial x_1}+\frac{\omega\beta(1+\alpha_m x_0)}{(\omega^2-1)\alpha_m}\frac{\partial}{\partial z_1}+\left[\frac{\omega^4-\omega^2+1}{(\omega^2-1)(2\omega^2-1)\alpha_m}+\frac{\omega^2 x_0}{\omega^2-1}\right]\frac{\partial}{\partial t_1}\right]N_g a_g$$
$$\times\exp(\alpha_m x_0)\exp[i(\beta z_0-\omega t_0)]-\frac{i\beta N_g^2 a_g^2}{(\omega^2-1)(4\omega^2-1)}\exp(2\alpha_m x_0)\exp[i2(\beta z_0-\omega t_0)]$$
$$+\frac{i\omega\alpha_{m1}}{\omega^2-1}g_1\exp(\alpha_{m1}x_0)\exp\{i[(\beta-K)z_0-\omega t_0]\}+\frac{i\omega\alpha_{m2}}{\omega^2-1}g_2\exp(\alpha_{m2}x_0)\exp\{i[(\beta+K)z_0-\omega t_0]\}$$
$$+\frac{i2\omega\alpha_{2m}}{4\omega^2-1}g_3\exp(\alpha_{2m}x_0)\exp[i2(\beta z_0-\omega t_0)]+\text{c.c.},\qquad\text{(C6)}$$

$$V_{x2}=\left[\frac{i\beta x_0}{(\omega^2-1)}\frac{\partial}{\partial x_1}-\frac{1}{\omega^2-1}\left[1+\frac{\beta^2 x_0}{\alpha_m}\right]\frac{\partial}{\partial z_1}-\left[\frac{2\omega\beta}{(\omega^2-1)^2}+\frac{\omega\beta x_0}{(\omega^2-1)\alpha_m}\right]\frac{\partial}{\partial t_1}\right]N_g a_g$$
$$\times\exp(\alpha_m x_0)\exp[i(\beta z_0-\omega t_0)]+\frac{i2\omega\alpha_m N_g^2 a_g^2}{(\omega^2-1)(4\omega^2-1)}\exp(2\alpha_m x_0)\exp[i2(\beta z_0-\omega t_0)]$$
$$-\frac{i(\beta-K)}{\omega^2-1}g_1\exp(\alpha_{m1}x_0)\exp\{i[(\beta-K)z_0-\omega t_0]\}-\frac{i(\beta+K)}{\omega^2-1}g_2\exp(\alpha_{m2}x_0)\exp\{i[(\beta+K)z_0-\omega t_0]\}$$
$$-\frac{i2\beta}{4\omega^2-1}g_3\exp(\alpha_{2m}x_0)\exp[i2(\beta z_0-\omega t_0)]+\text{c.c.},\qquad\text{(C7)}$$

$$V_{z2}=\left[-\frac{\alpha_m x_0}{\omega^2-1}\frac{\partial}{\partial x_1}-\frac{i\beta(1+\alpha_m x_0)}{(\omega^2-1)\alpha_m}\frac{\partial}{\partial z_1}+\left[\frac{i\omega}{(\omega^2-1)(1-2\omega^2)\alpha_m}-\frac{i\omega x_0}{\omega^2-1}\right]\frac{\partial}{\partial t_1}\right]N_g a_g$$
$$\times\exp(\alpha_m x_0)\exp[i(\beta z_0-\omega t_0)]-\frac{2\omega\beta N_g^2 a_g^2}{(\omega^2-1)(4\omega^2-1)}\exp(2\alpha_m x_0)\exp[i2(\beta z_0-\omega t_0)]$$
$$+\frac{\alpha_{m1}}{(\omega^2-1)}g_1\exp(\alpha_{m1}x_0)\exp\{i[(\beta-K)z_0-\omega t_0]\}+\frac{\alpha_{m2}}{\omega^2-1}g_2\exp(\alpha_{m2}x_0)\exp\{i[(\beta+K)z_0-\omega t_0]\}$$
$$+\frac{\alpha_{2m}}{4\omega^2-1}g_3\exp(\alpha_{2m}x_0)\exp[i2(\beta z_0-\omega t_0)]+\text{c.c.}, \quad \text{(C8)}$$

$$N_2=-\frac{2}{4\omega^2-1}N_g^2 a_g^2\exp(2\alpha_m x_0)\exp[i2(\beta z_0-\omega t_0)]\ . \quad \text{(C9)}$$

APPENDIX D: THIRD-ORDER FIELDS

The third-order fields that are needed in obtaining the enhanced second-harmonic specular reflection are given by

$$B_{y3}^{v}=N_{f-1}A_{3,-1}^{v}\exp(ik_{v2}x_0)\exp\{i[(2\beta-K)z_0-2\omega t_0]\}+A_{3,2}^{v}\exp(ik_{v-2}x_0)\exp\{i[(\beta-2K)z_0-\omega t_0]\}+\text{c.c.}, \quad \text{(D1)}$$

$$E_{x3}^{v}=\frac{2\beta-K}{2\omega}N_{f-1}A_{3,-1}^{v}\exp(ik_{v2}x_0)\exp\{i[(2\beta-K)z_0-2\omega t_0]\}$$
$$+\frac{\beta-2K}{\omega}A_{3,2}^{v}\exp(ik_{v-2}x_0)\exp\{i[(\beta-2K)z_0-\omega t_0]\}+\text{c.c.}, \quad \text{(D2)}$$

$$E_{z3}^{v}=-\frac{k_{v2}}{2\omega}N_{f-1}A_{3,-1}^{v}\exp(ik_{v2}x_0)\exp\{i[(2\beta-K)z_0-2\omega t_0]\}$$
$$-\frac{k_{v-2}}{\omega}A_{3,2}^{v}\exp(ik_{v-2}x_0)\exp\{i[(\beta-2K)z_0-\omega t_0]\}+\text{c.c.}, \quad \text{(D3)}$$

$$B_{y3}^{m}=A_{3,-1}^{m}\exp(\alpha_{m2-}x_0)\exp\{i[(2\beta-K)z_0-2\omega t_0]\}$$
$$+A_{3,2}^{m}\exp(\alpha_{m-2}x_0)\exp\{i[(\beta-2K)z_0-\omega t_0]\}+\text{c.c.}, \quad \text{(D4)}$$

$$E_{x3}^{m}=\frac{1}{4\omega^2-1}\left\{-\frac{[\alpha_m(\beta-K)-\alpha_{m1}\beta]K+(\alpha_m+\alpha_{m1})(\omega^2-1)}{(\omega^2-1)^2}N_g a_g g_1\right.$$
$$\left.\times\exp[(\alpha_m+\alpha_{m1})x_0]+2\omega(2\beta-K)A_{3,-1}^{m}\exp(\alpha_{m2-}x_0)\right\}\exp\{i[(2\beta-K)z_0-2\omega t_0]\}$$
$$+\frac{\omega(\beta-2K)}{\omega^2-1}A_{3,2}^{m}\exp(\alpha_{m-2}x_0)\exp\{i[(\beta-2K)z_0-\omega t_0]\}+\text{c.c.}\ , \quad \text{(D5)}$$

$$E_{z3}^{m}=\frac{1}{(4\omega^2-1)}\left\{-\frac{i(2\beta-K)[\beta(\beta-K)-\alpha_m\alpha_{m1}]}{(\omega^2-1)^2}N_g a_g g_1\exp[(\alpha_m+\alpha_{m1})x_0]\right.$$
$$\left.+i2\omega\alpha_{2m-}A_{3,-1}^{m}\exp(\alpha_{m2-}x_0)\right\}\exp\{i[(2\beta-K)z_0-2\omega t_0]\}$$
$$+\frac{i\omega\alpha_{m-2}}{\omega^2-1}A_{3,2}^{m}\exp(\alpha_{m-2}x_0)\exp\{i[(\beta-2K)z_0-\omega t_0]\}+\text{c.c.}, \quad \text{(D6)}$$

$$V_{x3}=\frac{1}{4\omega^2-1}\left\{\frac{i2\omega[\alpha_m(\beta-K)-\alpha_{m1}\beta]K+(\alpha_m+\alpha_{m-2})(\omega^2-1)}{(\omega^2-1)^2}N_g a_g g_1\right.$$
$$\left.\times\exp[(\alpha_m+\alpha_{m1})x_0]-i(2\beta-K)A_{3,-1}^{m}\exp(\alpha_{m2-}x_0)\right\}$$
$$\times\exp\{i[(2\beta-K)z_0-2\omega t_0]\}-\frac{i(\beta-2K)}{\omega^2-1}A_{3,2}^{m}\exp(\alpha_{m-2}x_0)\exp\{i[(\beta-2K)z_0-\omega t_0]\}+\text{c.c.}, \quad \text{(D7)}$$

$$V_{z3}=\frac{1}{(4\omega^2-1)}\left[-\frac{2\omega(2\beta-K)[\beta(\beta-K)-\alpha_m\alpha_{m1}]}{(\omega^2-1)^2}N_g a_g g_1\exp[(\alpha_m+\alpha_{m1})x_0]\right.$$
$$\left.+\alpha_{2m-}A^m_{3,-1}\exp(\alpha_{m2-}x_0)\right]\exp\{i[(2\beta-K)z_0-2\omega t_0]\}$$
$$+\frac{\alpha_{m-2}}{\omega^2-1}A^m_{3,2}\exp(\alpha_{m-2}x_0)\exp\{i[(\beta-2K)z_0-\omega t_0]\}+\text{c.c.}, \tag{D8}$$

$$N_3=\frac{1}{(\omega^2-1)^2(4\omega^2-1)}\left\{(\alpha_m+\alpha_{m1})K[\alpha_m(\beta-K)-\alpha_{m1}\beta]\right.$$
$$\left.+(\alpha_m+\alpha_{m1})^2(\beta^2-\alpha_m^2)-(2\beta-K)^2[\beta(\beta-K)-\alpha_m\alpha_{m1}]\right\}N_g a_g g_1$$
$$\times\exp[(\alpha_m+\alpha_{m1})x_0]\exp\{i[(2\beta-K)z_0-2\omega t_0]\}+\text{c.c.} \tag{D9}$$

Here we have assumed that the fields with the phase factor $\exp\{i[(\beta-2K)z_0-\omega t_0]\}$ is a propagating wave in vacuum. Otherwise, $K_{v-2}=[\omega^2-(\beta-2K)^2]^{1/2}$ should be replaced by $K_{v-2}=i\alpha_{v-2}=i[(\beta-2K)^2-\omega^2]^{1/2}$. The wave amplitudes $A^v_{3,-1}$ and $A^m_{3,-1}$ are given by Eqs. (50) and (48), respectively. The wave amplitudes $A^v_{3,2}$ and $A^m_{3,2}$ are given as

$$A^v_{3,2}=A^m_{3,2}+\eta\{4\alpha_{m1}g_1-[\eta(\alpha_m^2-\alpha_v^2)N_g a_g]-i4\eta N_f k_{v1}C_{rg}a_g\}/8+i\eta N_f k_{v1}(1-C_{rr})a_i/2\ , \tag{D10}$$

$$A^m_{3,2}=\frac{1}{2D_2}(\{i\eta\omega[K(\beta-K)-\alpha_{m1}^2]/(\omega^2-1)\}-\eta k_{v-2}\alpha_{m1}/\omega)g_1$$
$$\times\frac{a_g}{8\omega D_2}\{-\eta k_{v-2}(\alpha_m^2-\alpha_v^2)N_g-i4N_f k_{v-2}k_{v1}C_{rg}+i\eta\alpha_v(2K\beta-\alpha_v^2)N_g$$
$$-i4N_f[K(\beta-K)-k_{v1}^2]C_{rg}\}+\frac{i\eta^2\omega\alpha_m a_g(2K\beta-\alpha_m^2)}{8(\omega^2-1)}$$
$$-\frac{i\eta N_f a_i}{2\omega D_2}\{k_{v-2}k_{v1}(1-C_{rr})+[K(\beta-K)+k_{v1}^2](1+C_{rr})\}\ , \tag{D11}$$

where

$$D_2=\frac{[(\omega^2-1)k_{v-2}+i\omega^2\alpha_{m-2}}{\omega(\omega^2-1)}\ .$$

[1]Y. J. Chen, A. R. B. de Castro, and Y. R. Shen, Phys. Rev. Lett. **46**, 145 (1981).
[2]G. S. Agarwal and S. S. Jha, Phys. Rev. B **26**, 482 (1982).
[3]R. Reinisch and M. Neviere, Phys. Rev. B **28**, 1870 (1983).
[4]G. A. Farias and A. A. Maradudin, Phys. Rev. B **30**, 3002 (1984).
[5]T. Tsang and D. D. Smith, Opt. Commun. **70**, 115 (1989).
[6]W. M. Robertson, A. L. Moretti, and R. Bray, Phys. Rev. B **35**, 8919 (1987).
[7]*Surface Enhanced Raman Scattering,* edited by R. K. Chang and T. E. Furtak (Plenum, New York, 1982).
[8]S. Ushioda, J. E. Rutledge, and R. M. Pierce, Phys. Rev. B **34**, 6804 (1986).
[9]S. M. Arakelian *et al.,* Phys. Lett. A **145**, 49 (1990).
[10]P. Beckmann and A. Spizzichno, *The Scattering of Electromagnetic Waves From Rough Surfaces* (Pergamon, New York, 1963).
[11]G. Li and S. R. Seshadri, J. Opt. Soc. Am. B **6**, 1125 (1989).
[12]G. Li and S. R. Seshadri, J. Opt. Soc. Am. B **7**, 998 (1990).
[13]J. C. Quail and H. J. Simon, J. Opt. Soc. Am. B **5**, 325 (1988).
[14]N. Bloembergen, R. K. Chang, S. S. Jha, and C. H. Lee, Phys. Rev. **174**, 813 (1968).
[15]S. R. Seshadri, J. Appl. Phys. **59**, 1187 (1986).
[16]H. Raether, in *Surface Polaritons,* edited by V. M. Agranovich and D. L. Mills (North-Holland, Amsterdam, 1982), pp. 331–403.